

AD-A104 588

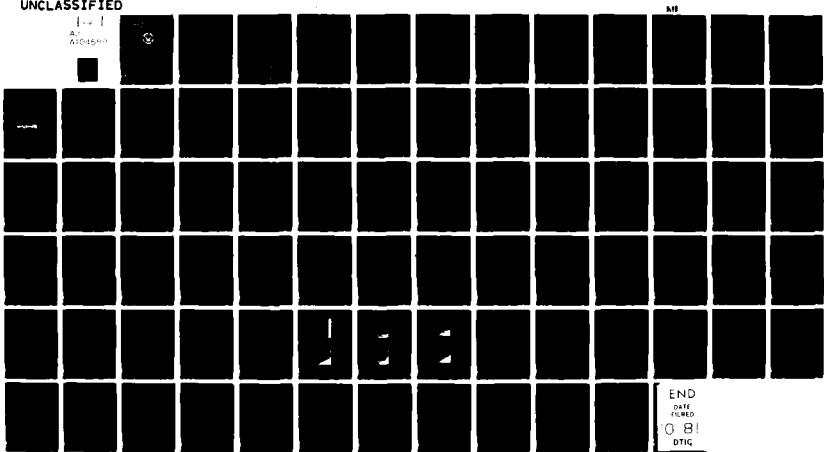
NAVAL POSTGRADUATE SCHOOL MONTEREY CA
FOURIER ANALYSIS OF BROADBAND, LOW-LEVEL SIGNALS USING SWITCHED--ETC(IU)
JUN 81 G L HOWARTH

F/6 9/3

UNCLASSIFIED

MF

AM
ADASAN



END
FILE
FURNISHED
0 81
DTIG

② LEVEL II

NAVAL POSTGRADUATE SCHOOL
Monterey, California

ADA104588



SDTIC
ELECTED
SEP 26 1981

B

THESIS

FOURIER ANALYSIS OF BROADBAND, LOW-LEVEL SIGNALS
USING SWITCHED INPUTS

by

Gary L. Howarth

June 1981

Thesis Advisor:

G. A. Myers

Approved for public release; distribution unlimited.

DTIC FILE COPY

81 9 28 028

UNCLASSIFIED

SECURITY CLASSIFICATION OF THIS PAGE (When Data Entered)

DD FORM 1 JUN 73 1473

EDITION OF 1 NOV 68 IS OBSOLETE
S/N 0102-014-66011

UNCLASSIFIED

SECURITY CLASSIFICATION OF THIS PAGE (When Data Entered)

UNCLASSIFIED

SECURITY CLASSIFICATION OF THIS PAGE/WHEN THIS PAGE WAS ENCODED.

#20 - ABSTRACT - (CONTINUED)

difference is formed and statistical analyses applied to determine statistically significant terms. The significant components comprise the estimate of the spectrum of the signal.

Analytical results are derived for sinusoidal signals and uncorrelated, Gaussian noise. Experimental results for both narrow and wideband signals and additive Gaussian noise are presented. Reasonable spectral estimates of a wideband signal are obtained with 16 averages when the composite signal-to-noise ratio is 0 dB.

Accession For	
NTIS GRAIL	<input checked="" type="checkbox"/>
DTIC TAB	<input type="checkbox"/>
Unclassified	<input type="checkbox"/>
Classification	<input type="checkbox"/>
Excluded From Distribution	<input type="checkbox"/>
Excluded From Public Release	<input type="checkbox"/>
Approved For Public Release	<input type="checkbox"/>
Approved For Public Release Date	<input type="checkbox"/>

A

Approved for public release; distribution unlimited.

Fourier Analysis of Broadband, Low-level Signals
Using Switched Inputs

by

Gary L. Howarth
Lieutenant Commander, United States Navy
B.S.M.E., Northwestern University, 1969

Submitted in partial fulfillment of the
requirements for the degree of

ELECTRICAL ENGINEER

from the

NAVAL POSTGRADUATE SCHOOL

June 1981

Author: Gary L. Howarth

Approved by: Brian A. Dwyer

Thesis Advisor

Stephen J. Kimball

Second Reader

DeKirk Chairman, Department of Electrical Engineering

William M. Jolley Dean of Science and Engineering

ABSTRACT

A new technique for estimation of the spectrum of an unknown signal is investigated. The technique combines a radiometric method of signal detection (modulating the receiver noise with the assumed signal by alternately connecting and disconnecting the input transducer) with a Fast Fourier Transform processor for spectral analysis. After obtaining averaged spectral estimates with the transducer (antenna) connected and disconnected the difference is formed and statistical analyses applied to determine statistically significant terms. The significant components comprise the estimate of the spectrum of the signal.

Analytical results are derived for sinusoidal signals and uncorrelated, Gaussian noise. Experimental results for both narrow and wideband signals and additive Gaussian noise are presented. Reasonable spectral estimates of a wideband signal are obtained with 16 averages when the composite signal-to-noise ratio is 0 dB.

TABLE OF CONTENTS

I.	INTRODUCTION -----	11
II.	THE FABLUS PROCESS -----	20
	A. PROCEDURE -----	20
	B. PROCESSING ERRORS -----	25
III.	STATISTICAL METHODS -----	30
	A. METHOD I--DIFFERENCE OF MEANS -----	31
	B. METHOD II--MEANS ONLY -----	39
	C. OTHER METHODS -----	42
	D. REFERENCE CALCULATION -----	45
	E. SIGNAL-TO-NOISE RATIOS -----	47
IV.	EXPERIMENTAL RESULTS -----	49
	A. NARROWBAND RESULTS -----	49
	B. WIDEBAND RESULTS -----	58
V.	CONCLUSIONS -----	63
APPENDIX A:	THE DISCRETE FOURIER TRANSFORM -----	64
APPENDIX B:	DERIVATION OF STATISTICAL PROPERTIES FOR SINUSOIDAL SIGNAL AND UNCORRE- LATED, GAUSSIAN NOISE -----	68
APPENDIX C:	PROBABILITY OF DETECTION FOR SINU- SOIDAL SIGNAL AND UNCORRELATED, GAUSSIAN NOISE -----	75
LIST OF REFERENCES -----	77	
INITIAL DISTRIBUTION LIST -----	78	

LIST OF FIGURES

1.	Block diagram of Radiometer system -----	12
2.	Block diagram of switched FFT system -----	14
3.	Example of spectra when the signal is a square wave -----	16
4.	Sampling of the analog waveform -----	21
5.	Discrete Fourier Transform of sampled waveform --	22
6.	Squared Magnitude of DFT of sampled waveform ----	24
7.	Block diagram of FABLUS system -----	29
8.	Interactions of hypothesis selection -----	32
9.	Block diagram of detection Method I -----	35
10.	Probability density functions for Method I -----	37
11.	Probability of detection vs. bin signal-to-noise ratio -----	38
12.	Block diagram of detection Method II -----	41
13.	Probability density functions for Method II -----	43
14.	Block diagram of the procedure used to compute the reference results -----	47
15.	Probability of detection vs. bin signal-to-noise ratio, analytical and experimental data ----	53
16.	Ensemble size vs. bin signal-to-noise ratio -----	56
17.	Probability of detection vs. bin signal-to-noise ratio -----	57
18.	Spectrum of signal only and noise only based on average of 500 samples -----	59
19.	Estimated and measured spectra, ensemble size of 8, composite SNR of 0 dB -----	60
20.	Estimated and measured spectra, ensemble size of 16, composite SNR of 0 dB -----	61

LIST OF TABLES

1.	Summary of probability of detection results -----	18
2.	Probability of detection, ensemble size 8 -----	51
3.	Probability of detection, ensemble size 16 -----	52

LIST OF SYMBOLS AND ABBREVIATIONS

d	- Population mean of $R(mf_0)$
f	- Frequency
f_c	- A constant, frequency of a sinusoidal signal
f_0	- Frequency interval between DFT output values = $1/NT$
$j(t)$	- Switching waveform
$n(t)$	- Noise waveform
p	- Probability density function
q	- Frequency index of DFT
r	- Realization of random variable $R(mf_0)$
$s(t)$	- Signal waveform
s_c^2	- Sample variance of DFT output under signal plus noise conditions
s_N^2	- Sample variance of DFT output under noise only conditions
s_s^2	- Sample variance of random variable $R(mf_0)$
t	- Time
u	- Population mean of DFT output under noise only conditions
v	- Population mean of DFT output under signal plus noise conditions
$x(t)$	- A general time function
$x(iT)$	- Sampled version of $x(t)$
z_a	- Statistical coefficient
A	- A constant, peak amplitude of a sinusoidal signal
$Al(mf_0)$	- Error in $X(mf_0)$ due to aliasing
$Al_N(mf_0)$	- Error in $G_N(mf_0)$ due to aliasing

$Al_S(mf_0)$	- Error in $G_S(mf_0)$ due to aliasing
B	- Proportionality constant
Cv	- Critical value used to test hypothesis
D_0	- Decision that signal component under consideration is not present
D_1	- Decision that signal component under consideration is present
$G_C(f)$	- Power spectrum under signal plus noise conditions
$G_C(mf_0)$	- DFT output under signal plus noise conditions
$G_C'(mf_0)$	- Sampled version of $G_C(f)$
$G_N(f)$	- Power spectrum under noise only conditions
$G_N(mf_0)$	- DFT output under noise only conditions
$G_N'(mf_0)$	- Sampled version of $G_N(f)$
$G_S(f)$	- Power spectrum under signal only conditions
$G_S(mf_0)$	- DFT output under signal only conditions
H_0	- Hypothesis being tested
$J(f)$	- Fourier transform of $j(t)$
M	- Ensemble size, number of samples of signal plus noise and noise only taken to calculate a spectral estimate
N	- Number of sample points in DFT input data block
$N(f)$	- Fourier transform of $n(t)$
P_d	- Probability of detection
$R(mf_0)$	- $G_C(mf_0) - G_N(mf_0)$
$S(f)$	- Fourier transform of $s(t)$
T	- Time interval between samples of an analog waveform
$Tr(mf_0)$	- Error in $X(mf_0)$ due to truncation
$Tr_N(mf_0)$	- Error in $G_N(mf_0)$ due to truncation

$Tr_S(mf_0)$ - Error in $G_S(mf_0)$ due to truncation
 $X(f)$ - Fourier transform of $x(t)$
 $X(mf_0)$ - DFT of $x(iT)$
 $X'(mf_0)$ - Sampled version of $X(f)$
 α - False alarm rate
 σ_C^2 - Population variance of DFT output under signal plus noise conditions
 σ_N^2 - Population variance of DFT output under noise only conditions

I. INTRODUCTION

Wideband noise-like signals occur in various types of radio communications and radio ranging systems. In this report, we present a method of signal processing which provides a measure of the spectrum of a wideband signal. This method combines the technique of radiometry which is used to detect weak radio signals with the Fourier transform which defines the spectrum of an electrical signal.

For more than twenty years, radiometers have been used in radio astronomy and elsewhere to detect low power signals (weak stars). In a radiometer the receiving element (antenna) is alternately connected to and disconnected from the receiver as shown in Fig. 1. The received voltage is therefore alternately weak signal $s(t)$ plus noise $n(t)$ and noise only. Hence, the receiver noise serves as a "carrier" which is then amplitude modulated by the weak signal by virtue of the switching action. Typically, a square-law device is used to demodulate the carrier. The square-law detector makes the system a power detector. Integration provides energy detection capability. The output from the energy detector alternately represents the energy level with no signal present (antenna disconnected) and the energy level when it is possible that a signal is present (antenna connected). The two values are compared using appropriate statistical analysis and a decision is made concerning the presence or absence of a signal. [Ref. 1]

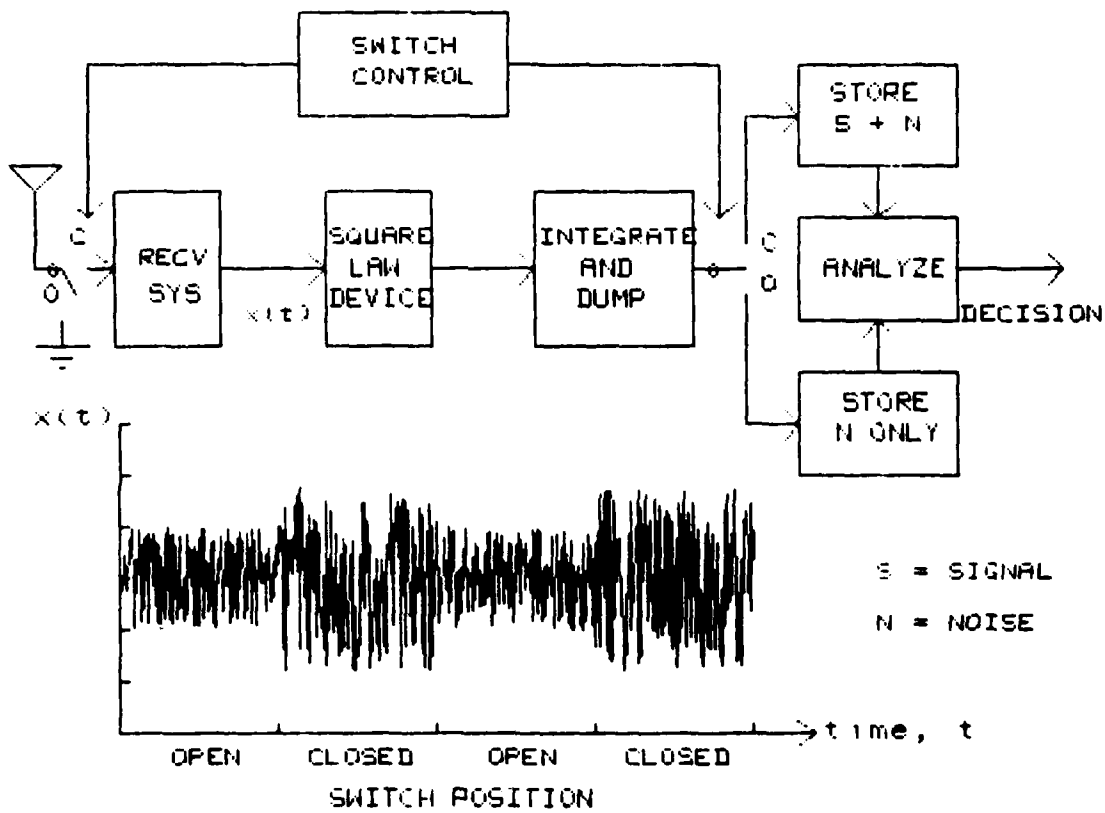


Fig. 1. Block diagram of a radiometer system.

So, the use of the receiver's own noise as a reference makes possible the detection of weak signals when the system noise is predominantly receiver noise (thermal noise-limited receivers). [In general, systems are thermal-noise limited if the frequencies of interest exceed 20 MHz.] Our interest is in the measurement of the spectra of weak signals. Replacing the square-law detector of Fig. 1 with a Fourier transform processor results in the system of Fig. 2. (In a practical system, the receiving subsystem of Fig. 2 includes a mixer so that the FFT processor operates on a lowpass or baseband portion of the spectrum.)

In this report, the processor of Fig. 2 includes a sampler which then allows use of the Fast Fourier Transform (FFT) algorithm to generate a discrete form of the spectrum of the processor input voltage. The FFT processor output is manipulated to produce an array of numbers proportional to the power at discrete frequencies, (the discrete power spectrum of the input). An average over M blocks of input data is formed which provides an output proportional to the energy of the input.

Because of the switching action at the system input, the FFT processor output alternately represents the spectrum $G_N(f)$ of the noise and the spectrum $G_C(f)$ of the combination of signal and noise. For the case of additive noise uncorrelated with the signal, we can write the signal spectrum $G_S(f)$ as $G_C(f) - G_N(f)$. Therefore, by subtracting the averaged spectra obtained with the FFT processor, a measure of the

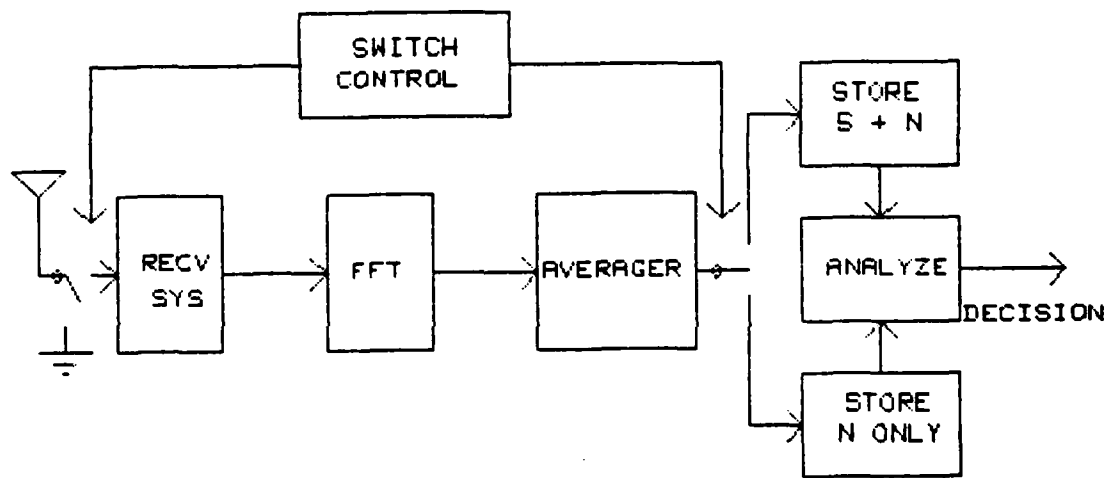
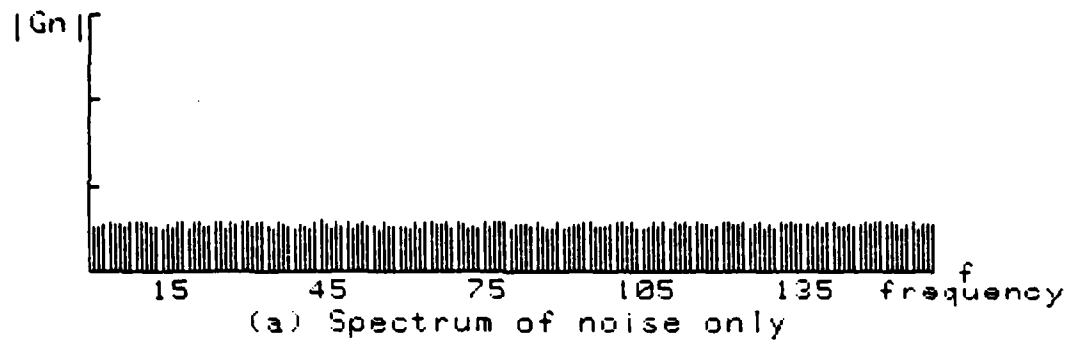


Fig. 2. Block diagram of switched FFT system.

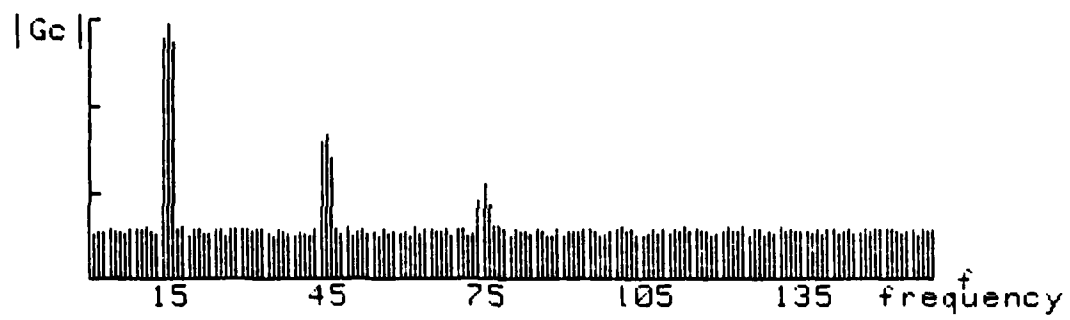
spectrum of the signal is formed when a signal is present. A near-zero difference indicates the absence of a signal. Fig. 3a shows the spectrum $G_N(f)$ of the noise only, Fig. 3b shows the spectrum $G_C(f)$ of the combined signal and noise for a square wave signal, and Fig. 3c shows the difference $G_S(f)$. Statistical analyses relate the number of blocks of data used in averaging to false alarm rate and detection probabilities. In this manner, the significant values of the difference (signal) spectrum are determined. Fig. 3c shows that the seventh and higher order harmonics of the square wave are missing from the spectral estimate. This is because the energy content of the higher order harmonics cannot be discerned from the energy content of the noise. Fig. 3c also shows two components which are not part of the spectrum of the signal (one at approximately 30 and another at approximately 150). These are caused by false alarms in the statistical analysis.

In this report, we identify this method with the acronym FABLUS (Fourier Analysis of Broadband, Low-level Signals Using Switching).

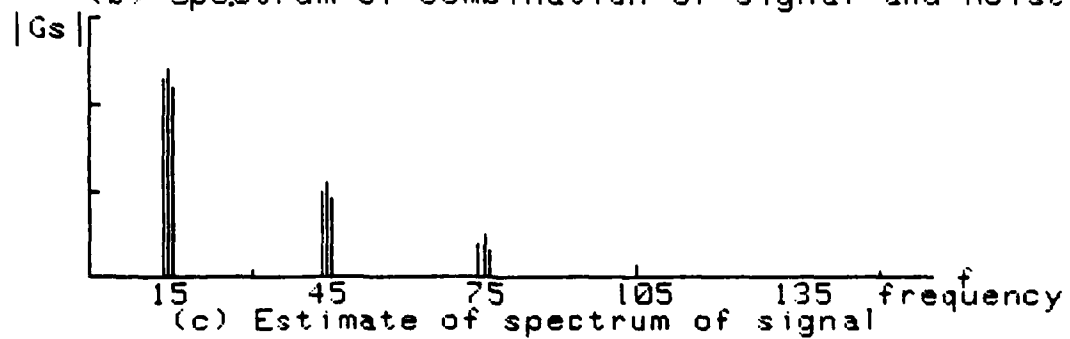
The FABLUS method of estimating signal spectra is useful when the receiver noise limits system performance. Noise which appears at the antenna (transducer) terminals is treated as signal. For accurate estimates of signal spectrum this method also requires the noise to be stationary over the interval of time required to obtain all the data used in calculating the



(a) Spectrum of noise only



(b) Spectrum of combination of signal and noise



(c) Estimate of spectrum of signal

Fig. 3. Example of spectra when the signal is a square wave

averages of the spectra of noise and combination of signal and noise. When these two conditions are satisfied, there is no theoretical limit on the level of a signal which can be detected and the accuracy with which the spectrum can be measured. By averaging over a large number of blocks of data (many ensembles or many cycles of the switch), the spectrum of a comparatively very weak signal can be accurately measured by this method.

Table 1 is an example of the results obtained using this method. Shown is the probability of detecting a signal component as a function of the ensemble size M and the ratio of the average signal amplitude to the average of the noise amplitude (frequency interval signal-to-noise ratio) when the false alarm rate is 2.5 percent.

The concept of signal-to-noise ratio requires definition when using the discrete Fourier transform. For example, if one watt of white, Gaussian noise (bandlimited to the processor bandwidth) is applied to an FFT processor which uses a 1024 sample block length the output will contain $1/512$ watts in each frequency interval. If a one watt sinusoidal signal, centered on one of the frequency intervals, is applied to the processor the output at the interval under consideration will contain one watt of power. The signal-to-noise ratio at this interval is $1/(1/512)$ or 27.1 dB. However, the signal-to-noise ratio at the input to the processor is $1/1$ or 0 dB. So, in evaluating the performance of a detection method, care

Table 1. Summary of probability of detection results.

Probability of Detection (%)

Ensemble Size (M)	Bin Signal-to-Noise Ratio			
	+10	0	-2	-8
8	100	30	16	4
16	100	51	28	6

must be used in defining the signal-to-noise ratio. All of the signal-to-noise ratios contained in this report are frequency interval (bin) signal-to-noise ratios based on a block length of 1024.

Chapter II of this report contains a detailed discussion of FABLUS including analysis of the errors associated with application of the FFT and the operations necessary to produce the arrays of numbers representing the energy content of noise only and combination of signal and noise. Chapter III discusses the statistical techniques investigated to determine the significance of the spectral components. Experimental results obtained using FABLUS are contained in Chapter IV. Chapter V presents conclusions. Derivations of analytical results are contained in Appendices A, B and C. A list of references is provided.

II. THE FABLUS PROCESS

A. PROCEDURE

Since the FFT processor is a digital device, the analog input voltage must be sampled and quantized. Fig. 4 shows an analog waveform $x(t)$ and the sampling operation. (The errors caused by quantization are not addressed in this report.) The sampling interval T and the number N of sample points in a data record are values which must be chosen carefully if the FFT processor output is to represent the spectrum of the input. Appendix A contains a brief review of Fourier transform theory and the Discrete Fourier Transform (DFT).

The output of the FFT processor is shown in Fig. 5 where $X(mf_0)$ represents the discrete Fourier transform of $x(t)$; m is the set of integers. The output consists of N complex numbers; however, only the first $N/2$ are unique. The spectra is "folded" about the $N/2$ value. Therefore, the usable output consists of $N/2$ complex numbers representing the inphase and quadrature components of the transform. These components are the transform values at discrete frequencies at intervals of $1/NT$ Hz in the range 0 to $1/2T$ Hz. We refer to an interval of $1/NT$ Hz as a frequency bin. We denote the output numbers by G_C when the combination of signal and noise is the input and by G_N when noise only is the input. These numbers vary from one block of data to the next because of the random nature of the input (random phase) relative to the switching

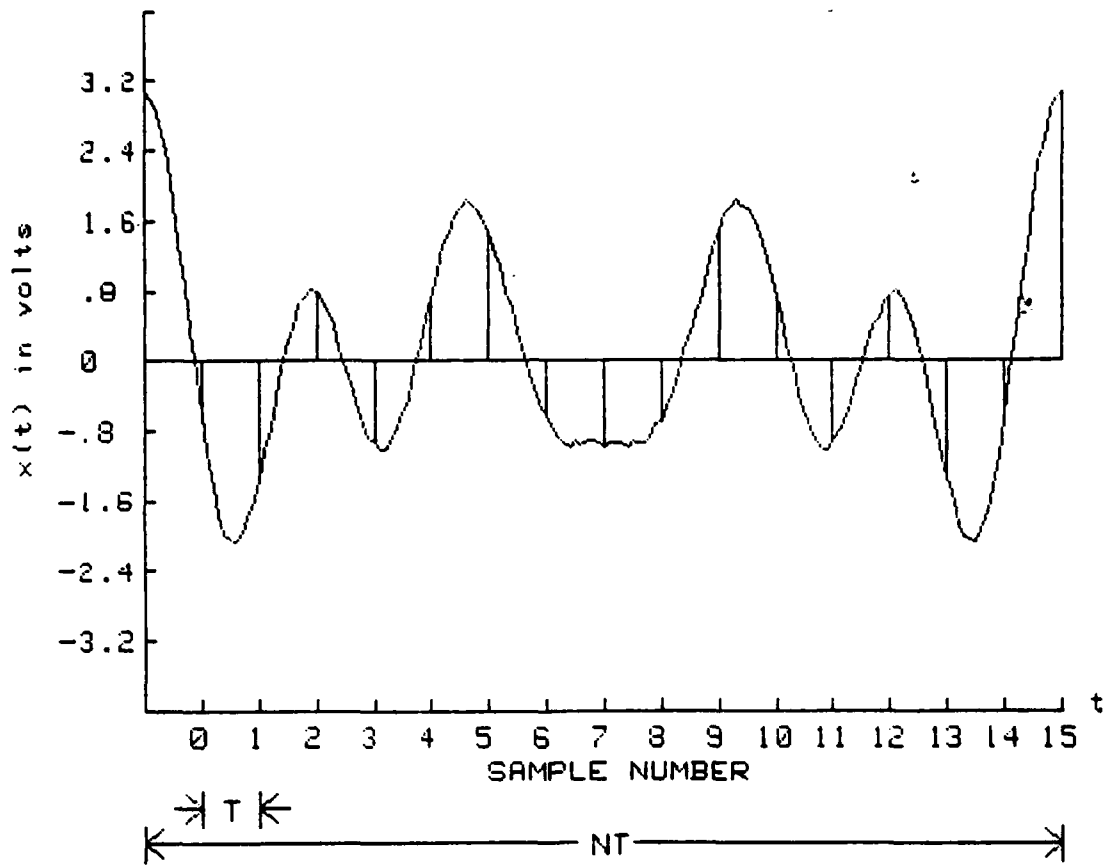


Fig. 4. Sampling of the analog waveform.

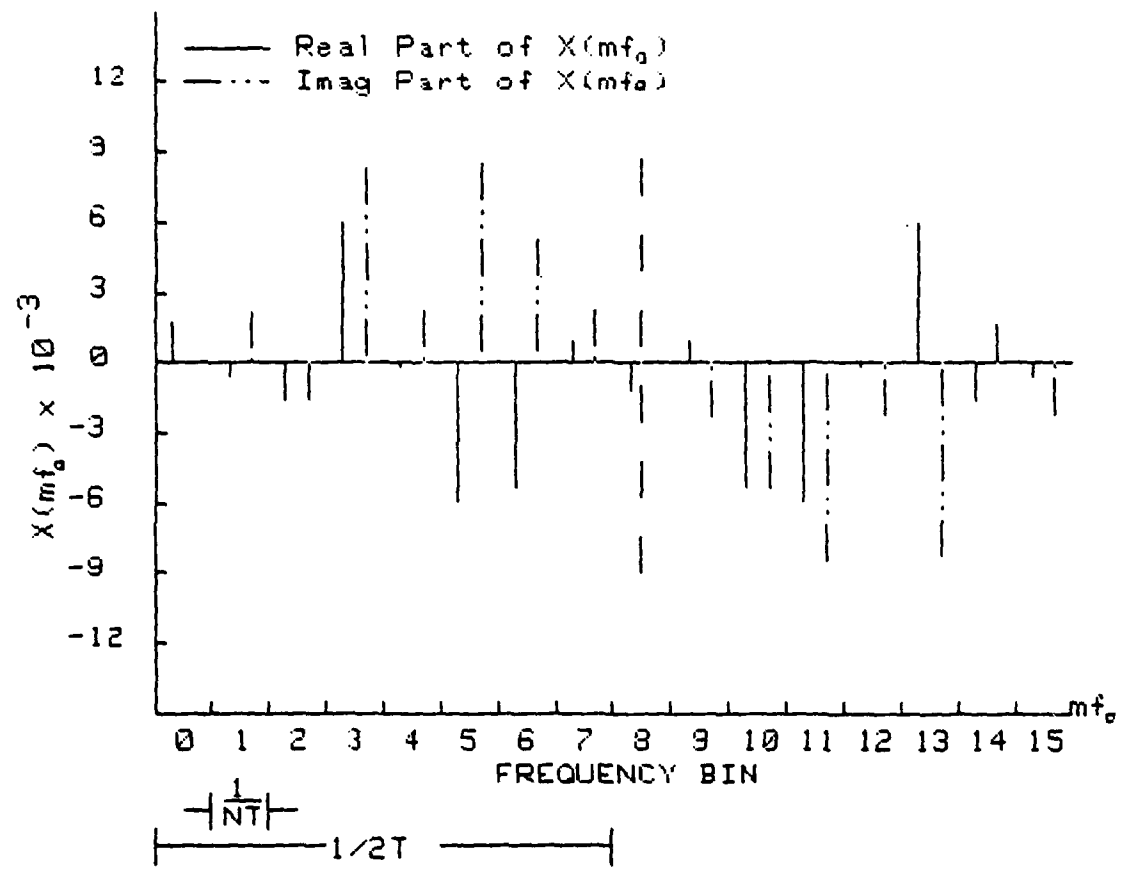


Fig. 5. Discrete Fourier Transform of sampled waveform.

and data truncation which is part of the FFT processor operation. To remove this randomness the squared magnitude of the transform $(\text{Re}(\))^2 + \text{Im}(\)^2$ is computed. The squared magnitudes are insensitive to phase variation and are proportional to the power contained in the input time record at each frequency bin. Fig. 6 shows the FFT output magnitude squared. Therefore, the first processing step is to convert the FFT output to magnitudes squared ($|G_C|^2$ and $|G_N|^2$) at each bin.

Averaging of M output arrays smooths the magnitude squared values and provides values proportional to energy for each bin. To perform the averaging, the sum of the magnitudes squared must be computed and stored after each block of input data has been processed. In addition to storing the sum of the magnitudes squared, the sum of the squares of the magnitudes squared ($[\|G_C\|^2]^2$ and $[\|G_N\|^2]^2$) is also stored to allow computation of the variance s_C^2 of the signal plus noise data and of the variance s_N^2 of the noise only data. Since the switching provides alternately noise only and a combination of signal and noise, a total of $2M$ blocks of data must be processed before computation of means ($\overline{|G_C|^2}$ and $\overline{|G_N|^2}$) and sample variances (s_C^2 and s_N^2) can be done. In the remainder of this report M will be referred to as ensemble size and will refer to the taking of a total of $2M$ samples of input voltage. These four arrays are the numerical output from which the estimate of the spectrum of the signal is formed. Appendix B contains derivations of $\overline{|G_C|^2}$, $\overline{|G_N|^2}$, s_C^2 and s_N^2 for the case of zero mean, white, Gaussian noise.

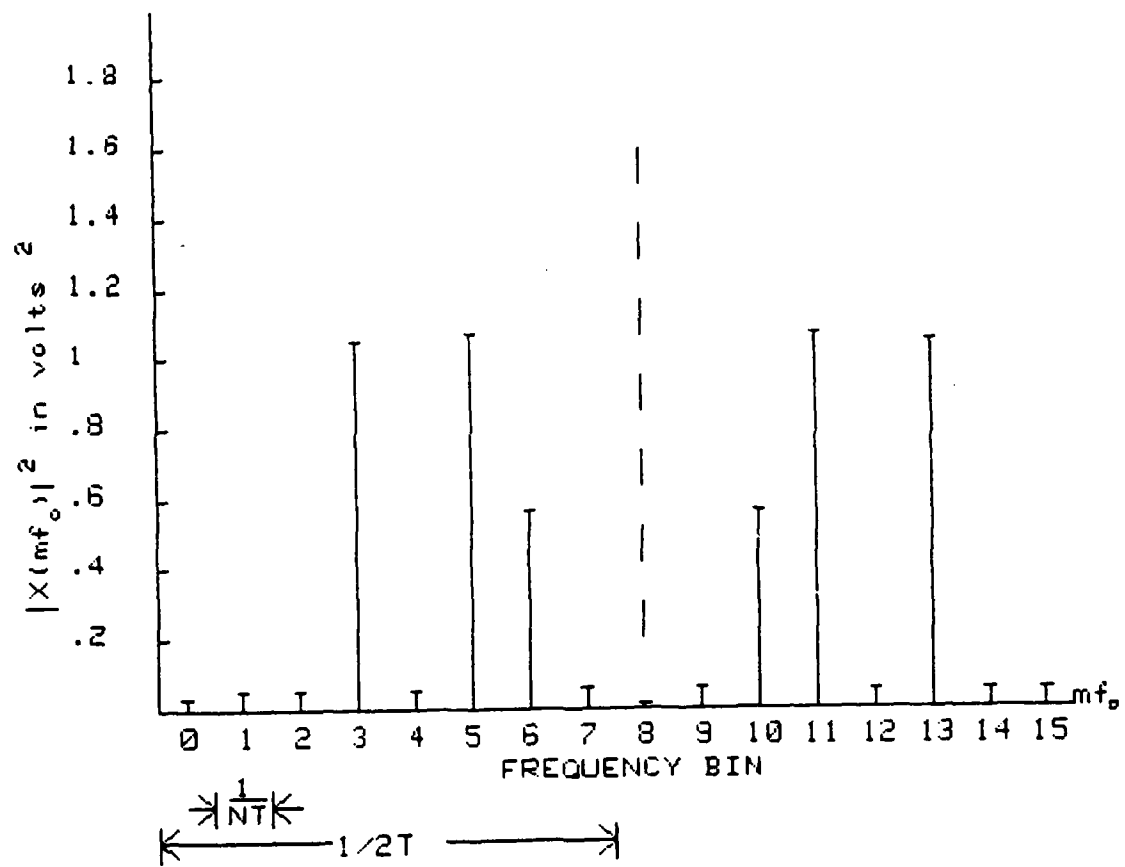


Fig. 6. Squared Magnitude of DFT of sampled waveform.

B. PROCESSING ERRORS

The output of the FFT processor contains the information necessary to estimate $G_S(f)$, the spectrum of $s(t)$. Variations in the arrays G_N and G_C due to random phase have been eliminated by using the transform magnitude squared. However, there are still four potential sources of error which could cause this estimate of $G_S(f)$ to differ from its true value. Three of these error sources are sampling of the input waveform, truncation of the input data record and the discrete nature of the output spectrum. These three are all associated with the FFT process. The fourth potential source of error is associated with the switching action necessary to produce the alternating inputs of noise only and combination of signal and noise.

Appendix A contains a discussion of the errors associated with estimating a continuous spectrum using an FFT processor. As derived there, the output of the FFT processor, with input $x(t)$ can be viewed as composed of three terms:

$$X(mf_0) = X'(mf_0) - Al(mf_0) - Tr(mf_0)$$

In this equation $X(mf_0)$ is the estimate of $X(f)$, $Al(mf_0)$ is the error caused by aliasing in the sampling of $x(t)$, $Tr(mf_0)$ is the error caused by truncation of the input data and $X'(mf_0)$ is the sampled replica of $X(f)$, the continuous spectrum; f_0 is the frequency interval = $1/NT$. If the input to the FFT processor is noise $n(t)$ only, the output will be

$$G_N(mf_0) = G_N'(mf_0) - Al_N(mf_0) - Tr_N(mf_0)$$

When the input is signal plus noise, $s(t) + n(t)$, the processor output becomes:

$$G_C(mf_0) = G_C'(mf_0) - Al_C(mf_0) - Tr_C(mf_0)$$

The errors due to aliasing in the signal plus noise output can be considered as composed of components associated with the noise (Al_N) and components associated with the signal (Al_S). If the signal and noise are uncorrelated, these two components will be independent and $Al_C(mf_0)$ can be written as $Al_S(mf_0) + Al_N(mf_0)$. Errors associated with the truncation of the input for signal plus noise conditions can also be written as two components $Tr_C(mf_0) = Tr_S(mf_0) + Tr_N(mf_0)$ because of the linearity of the Fourier transform. Form

$$\begin{aligned} R(mf_0) &= G_C(mf_0) - G_N(mf_0) \\ &= G_S'(mf_0) - Al_S(mf_0) - Tr_S(mf_0) + G_N'(mf_0) \\ &\quad - Al_N(mf_0) - Tr_N(mf_0) - G_N'(mf_0) + Al_N(mf_0) \\ &\quad + Tr_N(mf_0) \\ &= G_S'(mf_0) - Al_S(mf_0) - Tr_S(mf_0) \end{aligned}$$

This result shows that the errors caused by aliasing and truncation of the noise only waveform are eliminated when the difference is formed. Therefore, the computed difference represents the spectrum of the signal as if it had been applied

to the FFT processor without the noise. Since $R(mf_0)$ contains these erroneous frequency components which are not eliminated by the post transform processing, care must be exercised to minimize their effects. Careful choice of T , the sampling period, and N , the number of samples per block, will accomplish this.

One of the major features of this detection scheme is the switching of the antenna into and out of the receiver system input. This switching action can be modeled as a squarewave alternating between 0 and +1. Call this waveform $j(t)$. With $s(t)$ the signal and $n(t)$ the noise the FFT processor input $x(t)$ is:

$$x(t) = s(t)j(t) + n(t)$$

The multiplication of $s(t)$ by $j(t)$ produces discontinuities in $x(t)$. Multiplication in the time domain corresponds to convolution in the frequency domain. Denoting the convolution operation by $*$, we then have that the spectrum $X(f)$ of $x(t)$ is:

$$X(f) = S(f)*J(f) + N(f)$$

The convolution of $J(f)$ with $S(f)$ produces frequency components in $X(f)$ which are not in $S(f)$. However, these spurious components can be eliminated by blanking the FFT processor input during the transitions of $j(t)$. This will require that the record length of the processor input be slightly less than

the half period of $j(t)$ and that the FFT input blanking pulse and $j(t)$ be synchronized to allow the transients to decay sufficiently before the data is applied to the FFT processor. That is, the effects of switching are eliminated by selecting a complete block of data to be processed during the time interval the switch is closed.

In summary, the output of the FFT processor is an array of numbers representing an estimate of the spectrum of the processor input. This estimate is influenced by the phase variations of the data blocks relative to the signal, and by sampling, truncation and switching. The random phase variations are removed by computing the magnitude squared. The errors associated with the switching are removed by synchronization of the data taking and switching operations. Post transform processing (differencing) eliminates errors caused by sampling and truncation of the noise. The errors remaining in the post transform processed data are those associated with sampling and truncation of the signal $s(t)$. These are errors in the FFT process and are not caused by the switching action.

Fig. 7 is a more detailed block diagram of the FABLUS system.

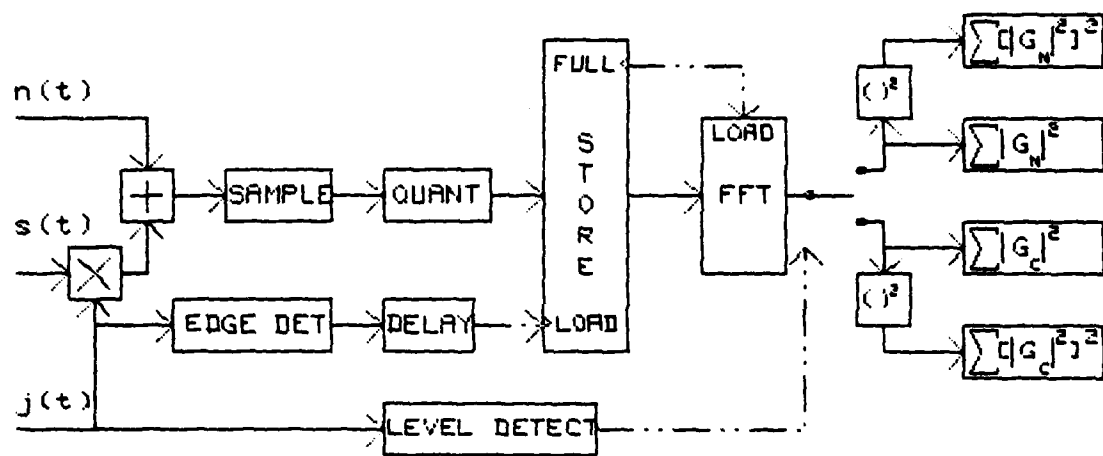


Fig. 7. Block diagram of the FABLUS system.

III. STATISTICAL METHODS

The output of the FFT processor is four arrays of numbers representing the sum of the squared magnitudes and the sum of the squared magnitudes squared (fourth power) at each frequency bin for noise only and signal plus noise inputs. The next step in the detection process is to manipulate these arrays to perform a statistical evaluation at each bin. The evaluation determines which bins contain statistically significant components. Those bins with significant components and the magnitudes of those components comprise the spectral estimate of $s(t)$.

There are at least two general courses of action available to perform the statistical analysis. First, it can be assumed that a signal is present and then evaluate the arrays to confirm or deny this hypothesis. Alternatively, it can be assumed that no signal is present and then evaluate the arrays to confirm or deny this hypothesis. These two approaches are not equivalent.

Hypothesizing that a signal is present requires some assumption about the level of that signal. This assumed level is the smallest which can be detected with the desired degree of confidence. Then, the statistical evaluation determines with $1-\alpha$ confidence that a signal of the assumed level or higher exists. This procedure sets a detection rate and a rate of missed detections.

Hypothesizing that no signal is present requires no assumptions about the signal level. The statistical evaluation determines with $1-\alpha$ confidence that no signal is present. This method sets the rate at which correct no signal decisions are made and the false alarm rate. The relation between these hypotheses, and the detection and false alarm rates are depicted in Fig. 8.

The no signal hypothesis requires no assumptions about signal level and setting of the false alarm rate. Unfortunately, the signal detection rate cannot be determined without signal level assumptions.

To minimize the number of assumptions required, the hypothesis no signal present is used in the signal detection methods employed here. This is in agreement with general practice where control of false alarm rate is usually preferred to control of signal detection rate. Various methods are investigated. The two most useful methods are first described in detail in the following.

A. METHOD I--DIFFERENCE OF TWO MEANS

This method requires fewest assumptions. The only assumption is that M (the number of samples used in acquisition of the arrays stored by the FFT processor) be large enough so the sample means ($\overline{|G_N|^2}$ and $\overline{|G_C|^2}$) are approximately Gaussian distributed and the sample variances (s_N^2 and s_C^2) are approximately the population variances (σ_N^2 and σ_C^2). Sample sizes as small as 10 or even less can meet the first requirement to reasonable accuracy. It is more difficult to predict the

		ACTUAL SIGNAL PRESENT	
		YES	NO
YES	DECISION	ACCEPT H_0 CORRECT DECISION (SIGNAL)	REJECT H_0' FALSE ALARM
SIGNAL			
PRESENT			
NO		REJECT H_0 MISSSED DETECTION	ACCEPT H_0' CORRECT DECISION (NO SIGNAL)

METHOD I H_0 : SIGNAL PRESENT

METHOD II H_0' : SIGNAL NOT PRESENT

Fig. 9. Interactions of hypothesis selection.

number of samples required to meet the second condition. Values of 30 or 40 are cited in some texts [Ref. 2,3]. However, since the population variances are unknown, no other reasonable action is available and this substitution is used for all values of M.

Under the assumptions listed above, the random variables $\overline{|G_N|^2}$ and $\overline{|G_C|^2}$ can be considered Gaussian with means u (the actual mean of the noise population) and v (the actual mean of the signal plus noise population) and variances σ_N^2/M and σ_C^2/M respectively. Form the random variable $R = \overline{|G_C|^2} - \overline{|G_N|^2}$ which is Gaussian distributed with mean $(v-u)$ and variance $((\sigma_C^2 + \sigma_N^2)/M)$. As indicated above the population variances must be replaced with the sample variances to yield:

Random Variable R: Normal $((v-u), (\overline{s_C^2} + \overline{s_N^2})/M)$

Without loss of generality we can assume that no signal is present ($v = u$) and make the null hypothesis $H_0: u = v$. The method proceeds as follows:

For each frequency bin i:

a.) Compute $\overline{|G_N|^2}_i$, $\overline{|G_C|^2}_i$, s_{Ni}^2 and s_{Ci}^2

b.) Compute $R_i = \overline{|G_C|^2}_i - \overline{|G_N|^2}_i$ and

$$s_{Si}^2 = (s_{Ci}^2 + s_{Ni}^2)/M$$

c.) Compute $Cv = z_\alpha s_{Si}$

where z_α = the standardized normal variable such that the area under this density function from z_α to ∞ equals α .

- d.) If $R_i < C_v$ accept H_0 and make decision $D_0 = \text{no signal at bin } i$.
- e.) If $R_i \geq C_v$ reject H_0 and make decision $D_1 = \text{signal present at bin } i$.
- f.) If H_0 is accepted set $R_i = 0$; spectral estimate does not have a component at i th bin.
- g.) If H_0 is rejected, then R_i is the estimate of the magnitude of the spectral component of the signal at bin i .

Fig. 9 is a block diagram of this method.

If no signal is present then the random variable R_i should have zero mean with variance $2s_{N_i}^2/M$ since the variance is the same for both sets of M samples. The probability density function for R_i conditioned on no signal is:

$$p(r|u=v) = \sqrt{M}/(2s_N \sqrt{\pi}) \exp(-Mr^2/4s_N^2)$$

where r is a value of the random variable R_i . The critical value is $z_\alpha \sqrt{2s_N^2/M}$. The region to the left of the critical value represents those values of R for which H_0 is accepted; to the right, H_0 is rejected. From this it is obvious that the choice of z_α sets the false alarm rate.

If a signal is assumed to be present, then $v-u = d$ and R_i has mean d and variance $(s_{C_i}^2 + s_{N_i}^2)/M$. The probability density function for R_i conditioned on a signal present is:

$$p(r|v-u=d) = \sqrt{M}/\sqrt{2\pi(s_{C_i}^2 + s_{N_i}^2)} \exp(-M(r-d)^2/2(s_{C_i}^2 + s_{N_i}^2))$$

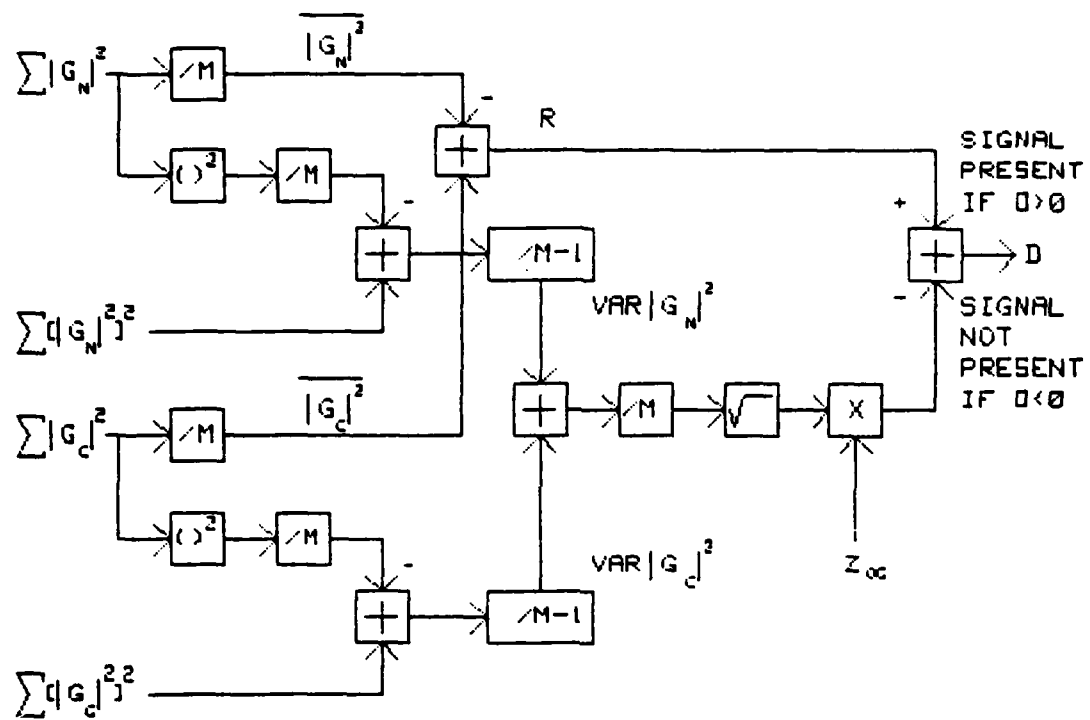


Fig. 9. Block diagram of detection Method I.

The critical value is not the same as in the no signal case because the variance of R is greater due to the signal. The probability of detection will be a function of d and s_S . The value of z_α is set by the false alarm rate. Fig. 10 is a graph showing both the no signal and signal present density functions.

To evaluate the analytical performance of this spectral estimation method, we apply the results from Appendix B to the procedure described above. The probability of detection for Method I is $P(r > Cv)$ where Cv is the critical value. This is evaluated in Appendix C for the case of sinusoidal signal and zero mean, white, Gaussian noise to give:

$$P(r > Cv) = Q(z_\alpha - (A^2 N^2 \sqrt{M}) / 4 \sqrt{(N^2 A^2 \bar{n}^2 / 2 + 2N^2 (n^2)^2)})$$

In this equation A is the peak amplitude of the sinusoidal signal, \bar{n}^2 is the mean square value of the noise process, M is the ensemble size, N is the number of points in the input data block and z_α is, as before, the value of the argument of the normal probability density function such that the area under the function from z_α to ∞ is α . The function $Q(x)$ is defined as the area under the standard normal density function from x to ∞ . Fig. 11 is a graph of probability of detection versus bin signal-to-noise ratio. From Fig. 11 we see that at 0 dB bin signal-to-noise ratio, the probability of detection increases by 22 percent (from 30 to 52) when the number M of records averaged is doubled (from 8 to 16).

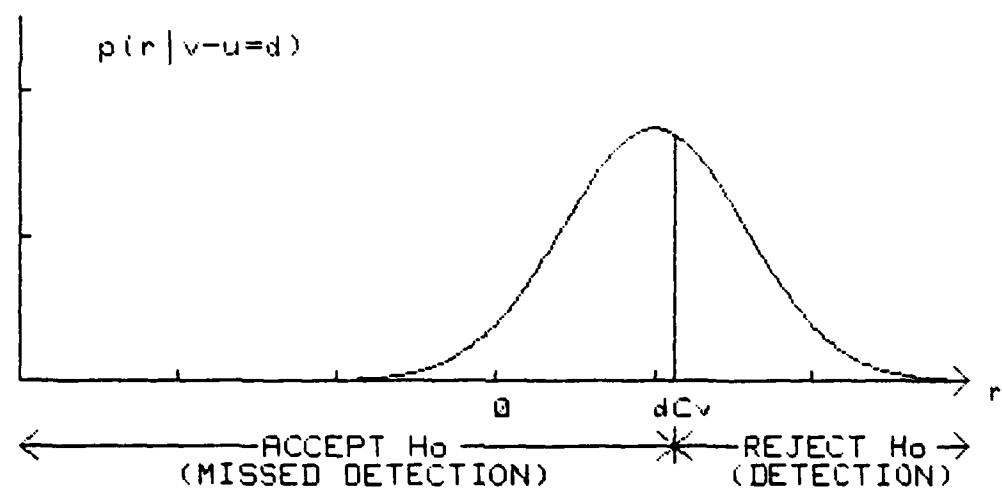
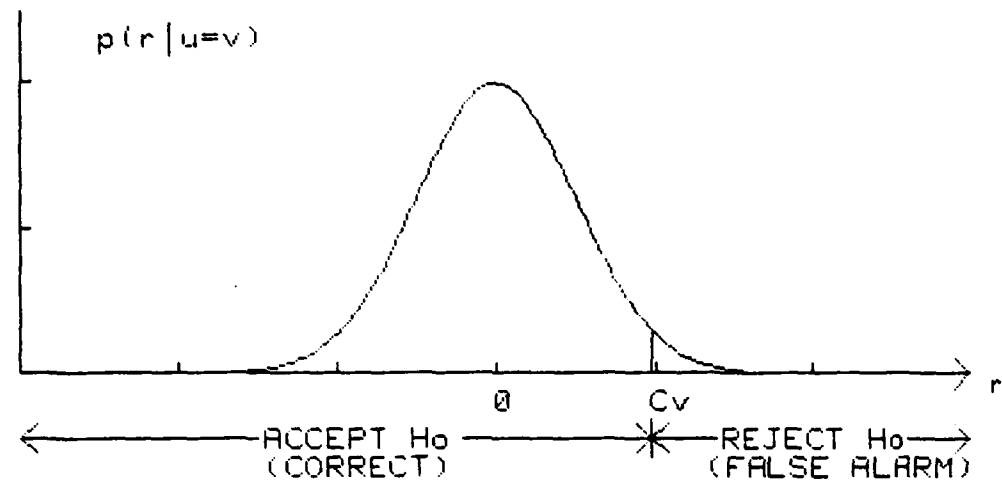


Fig. 10. Probability density functions for Method I.

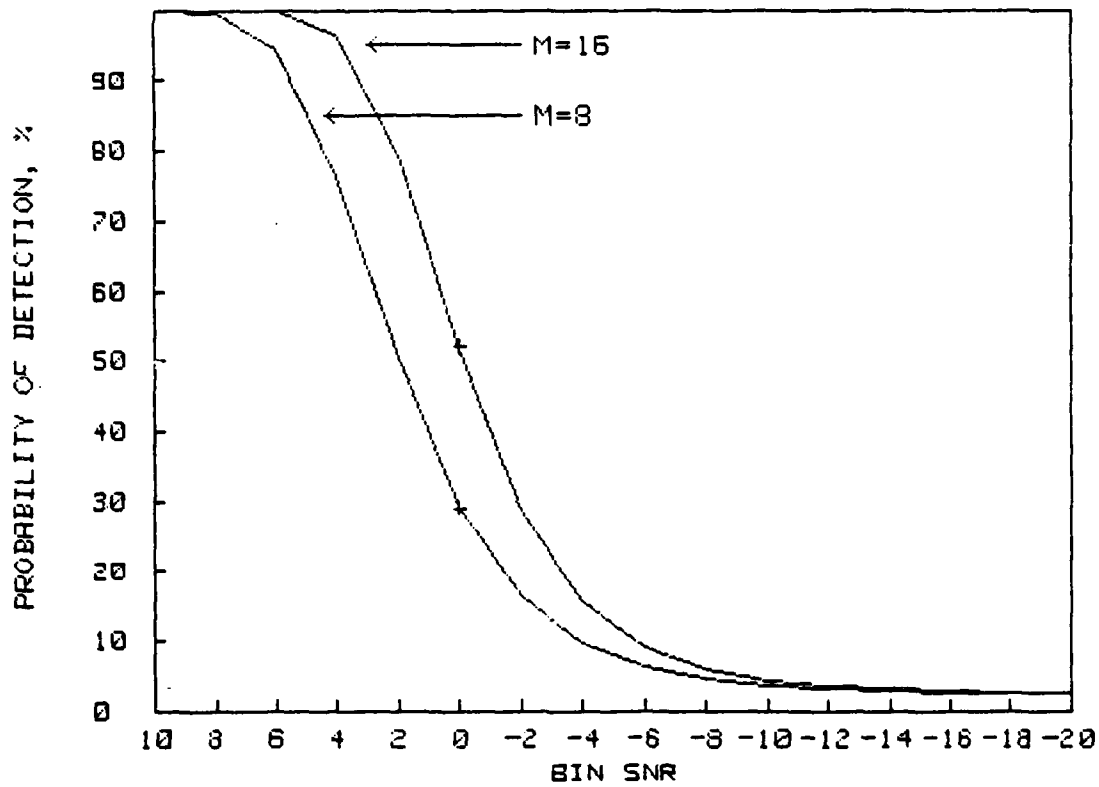


Fig. 11. Probability of detection vs. bin signal-to-noise ratio.

B. METHOD II--MEANS ONLY

Method I requires that the mean and variance of both the signal plus noise and the noise only ensembles be computed. These computations can be time consuming. Method II was developed to reduce the data and computation requirements. For this method only the mean values of the signal plus noise and noise only ensembles are required. However, the assumptions required are more restrictive than Method I. In addition to the assumption that the sample means are Gaussian distributed, it is assumed that a linear relationship exists between the standard deviation (s_N) of the noise only and the mean ($\overline{|G_N|^2}$) of the noise only, and that the variance of both ensembles are equal. That is, it is assumed $s_N = B \overline{|G_N|^2}$ and $\sigma_N^2 = \sigma_C^2$ where B is a constant.

It is difficult to identify cases where this linear relationship exists unless analytical methods are employed. Appendix A shows that for Gaussian, white noise these assumptions are valid with B = 1. The equal variance assumption is in general not valid; however, for small signal levels ($\sigma_S^2 \ll \sigma_N^2$), the error introduced is small.

Under these assumptions, the random variables $\overline{|G_N|^2}$ and $\overline{|G_C|^2}$ are Gaussian distributed with means u and v respectively and common variance σ_N^2 . Then the random variable $R_i = \overline{|G_C|^2} - \overline{|G_N|^2}$ is Gaussian with mean (v-u) and variance $2\sigma_N^2/M$. With the above assumptions we have:

$$\text{Random Variable } R: \text{Normal}((v-u), 2B^2(\overline{|G_N|^2})^2/M)$$

As in Method I we assume that $u = v$ and the null hypothesis

$H_0: u = v$.

For each frequency bin i :

a.) Compute $\overline{|G_C|_i^2}$ and $\overline{|G_N|_i^2}$

b.) Compute $R_i = \overline{|G_C|_i^2} - \overline{|G_N|_i^2}$ and

$$s_{Si} = \sqrt{sB} \overline{|G_N|_i^2} / \sqrt{M}$$

c.) Compute critical value $= Cv = z_\alpha s_{Si}$

d.) If $R_i < Cv$ accept H_0 and make decision $D_0 =$ no signal at bin i .

e.) If $R_i > Cv$ reject H_0 and make decision $D_1 =$ signal present at bin i .

f.) If H_0 is accepted set $R_i = 0$; spectral estimate does not have a component at i th bin.

g.) If H_0 is rejected, then R_i is the estimate of the magnitude of the spectral component of the signal at bin i .

Fig. 12 is a block diagram of the method.

Method II is basically the same as Method I. The only substantial difference is the method of establishing the variances and therefore the critical value.

Assuming no signal is present the decision variable R is Gaussian distributed with zero mean and variance $2s_N^2/M$. Therefore the probability density function of R conditioned on no signal is:

$$P(r|u=v) = \sqrt{M}/(2s_N\sqrt{\pi}) \exp(-r^2M/4s_N^2)$$

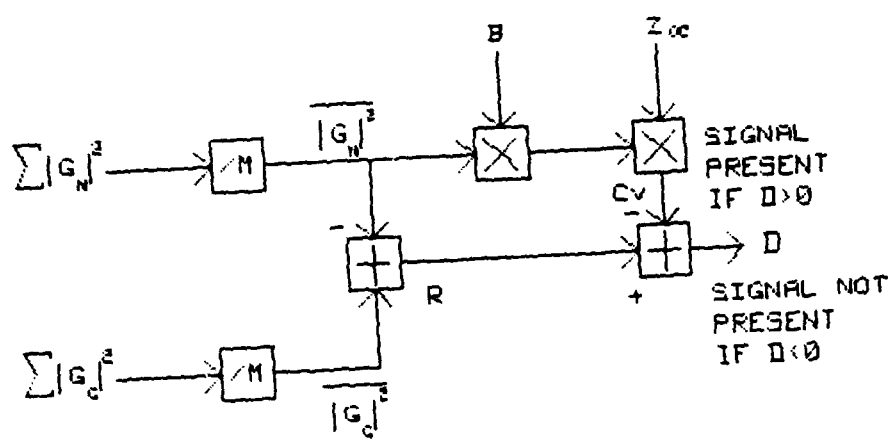


Fig. 12. Block diagram of detection Method II.

substituting $B|G_N|^2$ for s_N

$$P(r|u=v) = \sqrt{M}/(2B|G_N|^2\sqrt{\pi}) \exp(-Mr^2/(4B^2\{|G_N|^2\}^2))$$

The critical value will be:

$$Cv = z_\alpha \sqrt{2B|G_N|^2}/\sqrt{M}$$

Like Method I the area under the density function to the left of the critical value represents the probability of accepting H_0 (correct no signal decision). The area to the right represents the probability of incorrectly rejecting H_0 (false alarm).

If B is known exactly, then z_α will set the false alarm rate.

If a signal is present the decision variable R_i is Gaussian distributed with mean $(v-u)$. However, the variance is the same as in the no signal case. Therefore, the density function conditioned on signal present will be:

$$P(r|v-u=d) = \sqrt{M}/(2B|G_N|^2\sqrt{\pi}) \exp(-M(r-d)^2/4B^2\{|G_N|^2\}^2)$$

The area under the curve to the left of the critical value represents the probability of accepting H_0 (missed detection). The area to the right is the probability of correctly detecting the signal. In this case the probability of detection will be a function of d, B and $|G_N|^2$. Fig. 13 shows the density functions under signal and no signal conditions.

C. OTHER METHODS

In addition to the methods described above, we also investigated two methods which require the assumption that the

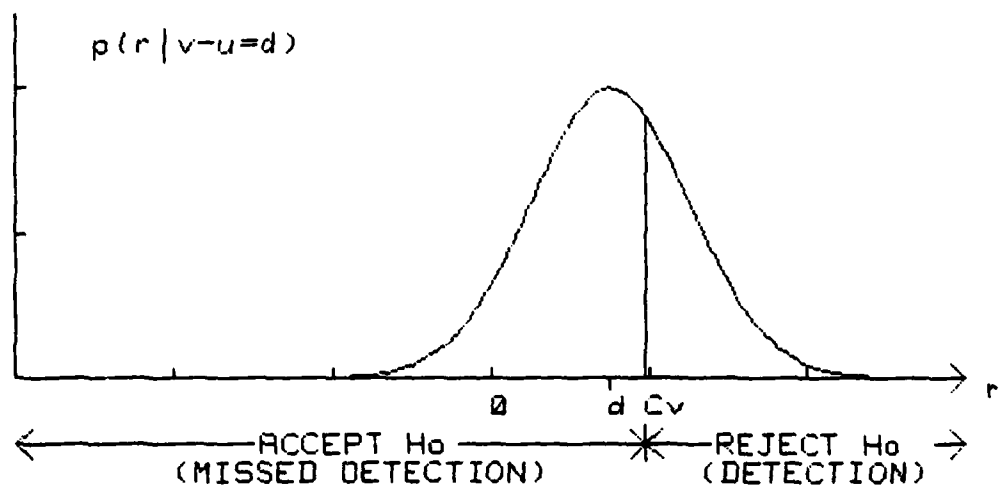
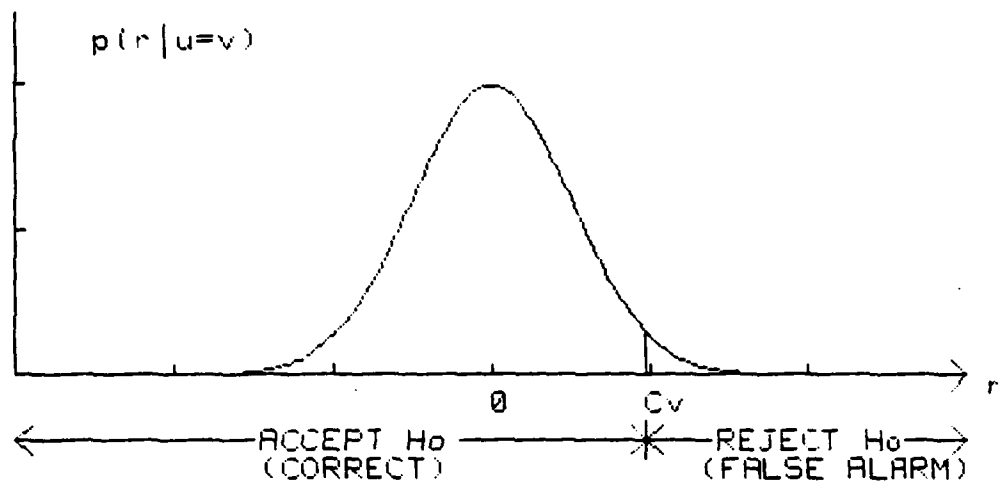


Fig. 13. Probability density functions for Method II.

population being sampled is Gaussian distributed. The two methods are Smith-Satterthwaite test for the difference of two means using Student t statistics and the ratio of two variances using F distribution statistics. The results for both these methods are significantly poorer than those of either Method I or II.

1. Smith-Satterthwaite Test--Difference of Means

This test suffered from two identified shortcomings. Unlike the two previous methods where the accuracy of the assumptions increased with increasing M, the validity of assuming the population being sampled is Gaussian distributed is not a function of M. Therefore, errors caused by using this assumption persist for any ensemble size. In addition, because the critical value is determined by calculating the degrees of freedom from the variance values, it is difficult to get consistent false alarm performance [Ref. 4].

2. F Distribution--Ratio of Variances

The ratio of two variances test also is afflicted with the errors caused by assuming the sampled population is Gaussian distributed. In addition the variability of the ratio of two variances is quite large at the relatively small ensemble sizes of interest here. This coupled with the rather large right hand tail of the F distribution causes the performance to be substantially worse than any of those already discussed [Ref. 5].

D. REFERENCE CALCULATION

One of the serious sources of error in Methods I and II is the variability of the critical value C_v . As long as the process is stationary the critical value should be a constant:

$$C_v = z_{\alpha} \sigma_C$$

Since the population variances are unknown, we use s_C as an estimate of σ_C . The changing value of C_v will cause errors in detection in addition to those due solely to the randomness associated with the decision variable R_i .

To gain insight into the amount of error caused by the changes in the critical value, this reference method was developed. To establish a constant critical value, the values of the variance of the noise and signal plus noise ensembles must be known exactly. To obtain a good estimate of these variances the statistics of both the noise and signal plus noise ensembles were collected during the testing of Methods I and II. This information was then evaluated to establish the values of σ_C^2 and σ_N^2 based on all the data taken during the tests. These numbers were used to calculate σ_C^2 . The computation proceeds as follows:

At each frequency bin i :

- a.) Compute $\overline{|G_S| i^2}$ and $\overline{|G_N| i^2}$
- b.) Compute $R_i = \overline{|G_S| i^2} - \overline{|G_N| i^2}$
- c.) Read in σ_C and compute $z_{\alpha} \sigma_C$

- d.) If $R_i < z_{\alpha} \sigma_C$ then accept H_0 ; no signal at bin i
- e.) If $R_i > z_{\alpha} \sigma_C$ reject H_0 ; signal present at bin i
- f.) If H_0 accepted set $R_i = 0$; spectral estimate has no component at bin i.

Because this method eliminates the errors caused by variability in the critical value, the detection results should be the best obtainable for a given signal level. Thus the detection results obtained with this method are used as a reference to compare the performance of Methods I and II. Fig. 14 is a block diagram of the computation process used to obtain the reference results.

E. SIGNAL-TO-NOISE RATIOS

The bin signal-to-noise ratio is the ratio of the average signal magnitude squared to the average noise magnitude squared ($\overline{|G_S|^2}/\overline{|G_N|^2}$) for a particular frequency bin. For the case considered above the signal-to-noise ratio is, from Appendix A,

$$\begin{aligned} \text{SNR}_1 &= A_N^2 / 4Nn^2 \\ &= A^2 N / 4n^2 \end{aligned}$$

This is a function of N, the input data block length, when using the FFT algorithm.

Alternatively an expression for the composite signal-to-noise ratio can be developed by solving

$$|G_N|^2 = \overline{Nn^2} \quad \text{and} \quad |G_S|^2 = A^2 N^2 / 4$$

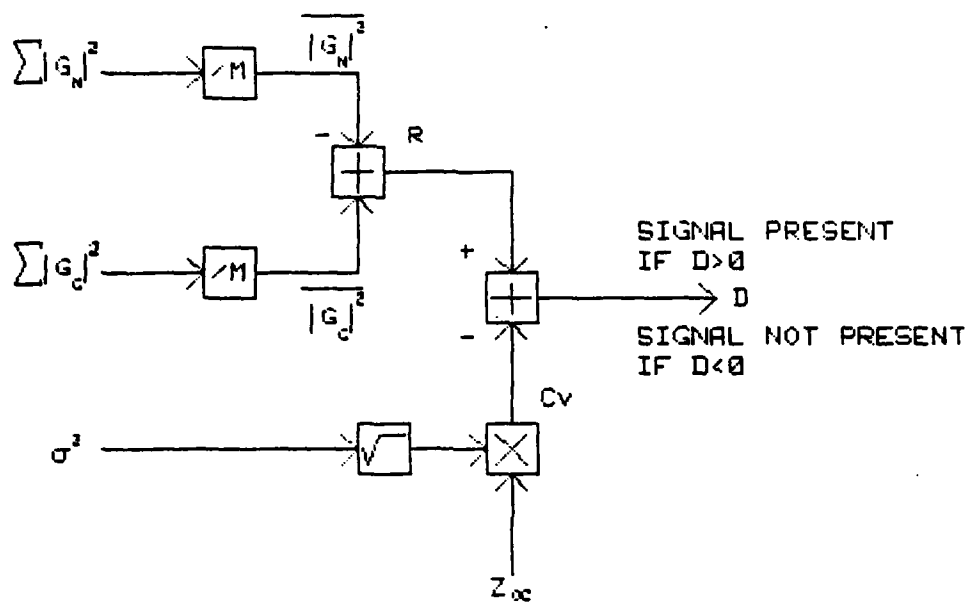


Fig. 14. Block diagram of the procedure used to compute the reference results.

for A^2 and \bar{n}^2 and forming:

$$\begin{aligned} \text{SNR2} &= A^2 / 2\bar{n}^2 \\ &= 2|G_S|^2 / N|G_N|^2 \end{aligned}$$

In this case the factor N is in the denominator whereas before it was in the numerator. For N = 1024 the following relationship exists between these alternative representations when SNR1 and SNR2 are in decibels and where $10 \log N/2 = 10 \log 512 = 27.1$.

$$\text{SNR2} = \text{SNR1} - 27.1 \text{ dB}$$

The expression shown for SNR1 is used throughout this report since the methods employed make spectral estimates on a bin-by-bin basis. Consequently, the noise power (or energy) at a particular frequency bin influences only the spectral estimate at that bin. Furthermore, in the general case of wideband, noise-like signals and non-Gaussian noise, SNR2 is not calculable because formulae for A^2 and \bar{n}^2 as functions of the average magnitudes squared are not known.

IV. EXPERIMENTAL RESULTS

A. NARROWBAND RESULTS

To demonstrate the capabilities of this method, a hardware evaluation was conducted using a signal generator, noise source, spectrum analyzer and minicomputer. A square wave signal was used to allow simultaneous processing of multiple signal levels. The noise source produced white, Gaussian noise. The spectrum analyzer did the sampling and obtained the FFT. The minicomputer provided the switching control, storage and computational capacity necessary to carry out the statistical analyses.

A total of 1000 trials was conducted with ensemble size M of eight. After each set of data was collected and the various sums computed, the values at the frequency bins containing the primary and third, fifth, seventh, ninth and eleventh harmonic frequencies of the input square wave were stored as well as data from five bins which contained no signal. After the 1000 trials were completed the data collected was analyzed using the previously described Methods I and II. A preliminary analysis was conducted using $z_{\alpha} = 1.96$ for Method I and $z_{\alpha} = 1.96$ and $B = 1$ for Method II (2.5 percent false alarm rate). Because of the variation in the validity of the assumptions used, the desired false alarm rate was not achieved. The value of z_{α} was then adjusted separately for each method until a 2.5 percent false alarm rate was achieved.

Next the data was reprocessed to determine the average values and variances at each bin over the 1000 trials. These averages and variances were then used to process the data to obtain the reference results. Table 2 shows the detection results for these trials.

The data obtained for the 1000 trials with $M = 8$ was then reprocessed to yield data for 500 trials with ensemble size 16. This data was then processed using Methods I, II and the reference procedure. These results are presented in Table 3.

The results for both the $M = 8$ and $M = 16$ trials are plotted in Fig. 15 along with the analytical probability of detection curves.

A comparison of the analytical and experimental results reveals that:

1. The analytical and experimental results for Method I agree very closely.
2. The reference results are substantially better than either Method I or II.
3. Method I is slightly better than Method II.

The very close agreement between the analytical and experimental results for Method I indicates that the assumption used (sample mean is Gaussian distributed) is generally valid for the case of white, Gaussian noise and sinusoidal signals. The results are not expected to change for other signal formats, since any waveform encountered in practice can be

TABLE 2. Probability of detection (%). Ensemble size 8,
false alarm rate 2.5%.

PROBABILITY OF DETECTION (%)

BIN SNR	METHOD I	METHOD II	REFERENCE
12.2	100	100	100
2.6	54.2	50.3	82.4
-2.2	13.2	11.7	23.9
-4.9	6.7	6.3	11.6
-7.2	3.3	4.1	6.3
-9.7	2.8	4.4	4.6

TABLE 3. Probability of detection (%). Ensemble size 16,
false alarm rate 2.5%.

PROBABILITY OF DETECTION (%)

BIN SNR	METHOD I	METHOD II	REFERENCE
12.2	100	100	100
2.6	88.2	84.6	99.8
-2.2	28.6	22.2	56.0
-4.9	12.6	12.6	23.6
-7.2	4.3	4.2	11.2
-9.7	5.4	6.2	7.0

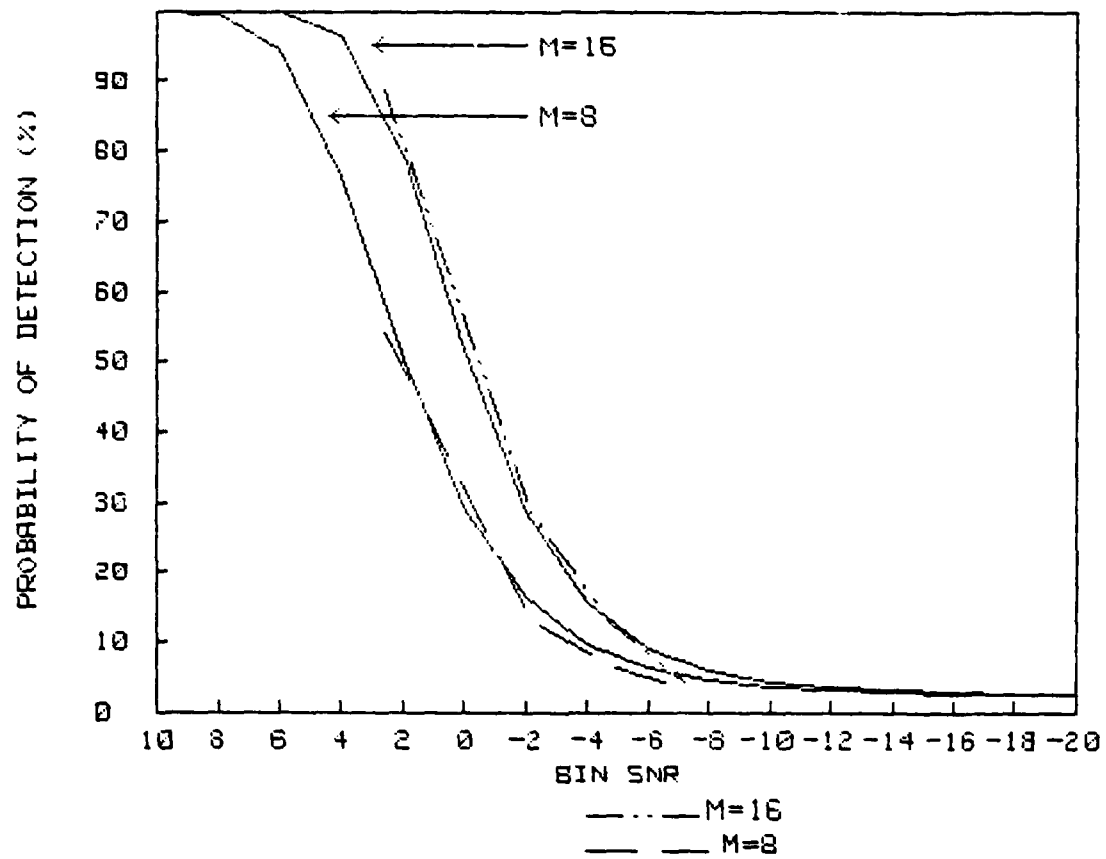


Fig. 15. Probability of detection vs. bin signal-to-noise ratio; analytical and experimental data.

expressed as a sum of sinusoids. The validity of the assumption for other types of noise is open to question. However, the ability of the method to detect the signals will not be greatly changed by the presence of non-Gaussian noise if the ensemble size is large enough to allow the Gaussian distributed sample mean assumption.

As expected the reference results show greater detection ability at all signal levels. They are included here only to indicate an upper limit of detection under these conditions. It may be difficult to implement such a method since it requires prior knowledge of the statistics of the processes involved.

A comparison of the probabilistic characteristics of Methods I and II (see Figs. 10 and 13) indicates that Method II should have higher probability of detection than Method I because the critical value will be less under otherwise identical conditions. However, the experimental results show precisely the opposite. The smaller critical value obtained using Method II is due to the use of the noise only data to compute the variance of R . The resulting smaller critical value does increase the probability of detection, but it also increases the false alarm rate. When the value of z_α is adjusted to regain the desired false alarm rate, the probability of detection decreases to the levels shown in Tables 2 and 3. The increase in the false alarm rate is not predicted by the analytical analysis but is due to additional noise entering

the experimental system along with the signal. This type of error can be encountered in any method where the critical value is calculated from noise only data. The use of both signal plus noise and noise only data to calculate the critical value, as in Method I, provides a limited amount of protection against this type of error.

The marginal increase in detection capability which Method I shows over Method II is probably due to the greater amount of information used in the Method I process. Since Method I uses both the means and variances to make spectral estimates, the extremes in the means may be counterbalanced to some extent by the variances. This might produce a smaller overall fluctuation in the decision variables. Method II uses the means to set the critical value and to compute the value of the decision variable. Therefore, this process would be more sensitive to the variations of the means.

However, the slightly increased detection capability of Method I does not occur without cost. Implementation of Method I requires additional computation time since the arrays of squared magnitudes squared must be computed and requires twice the storage capacity since four arrays must be stored instead of two.

A graph of ensemble size versus signal-to-noise ratio for 50 and 95 percent probability of detection is included as Fig. 16. Additionally, Fig. 17 is a graph of probability of detection versus bin signal-to-noise ratio for 2.5, 5 and 10

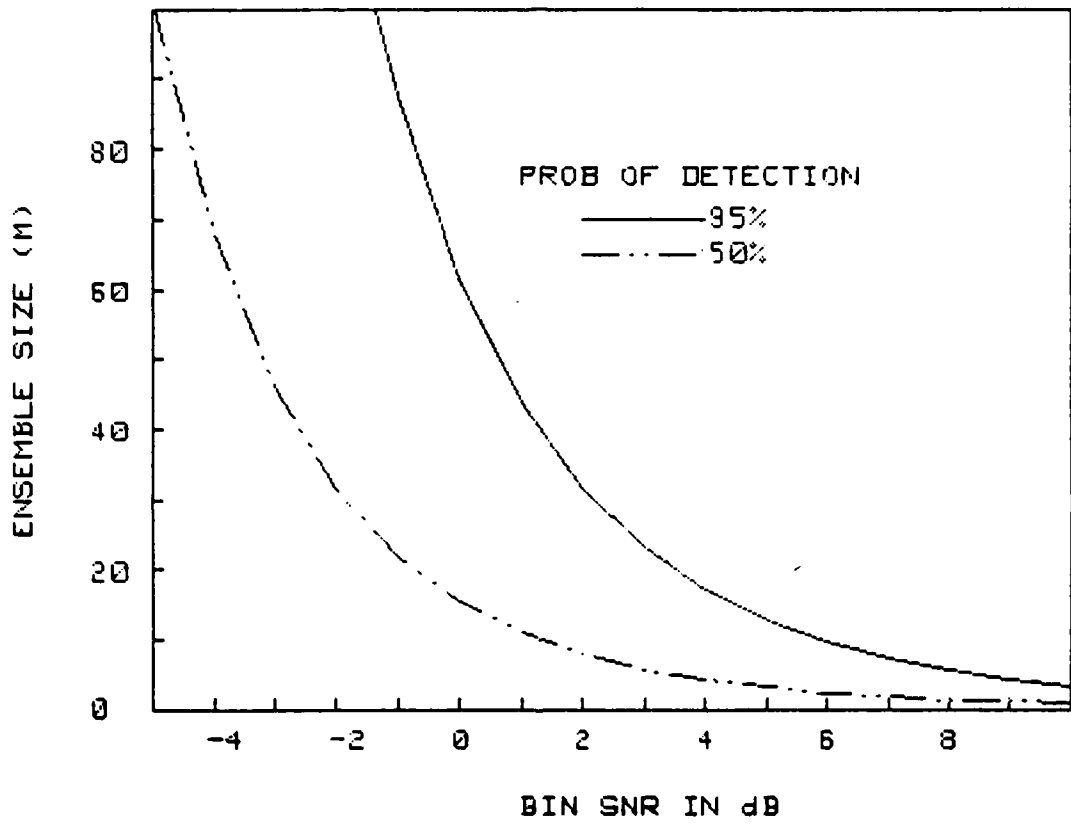


Fig. 16. Ensemble size vs. bin signal-to-noise ratio.

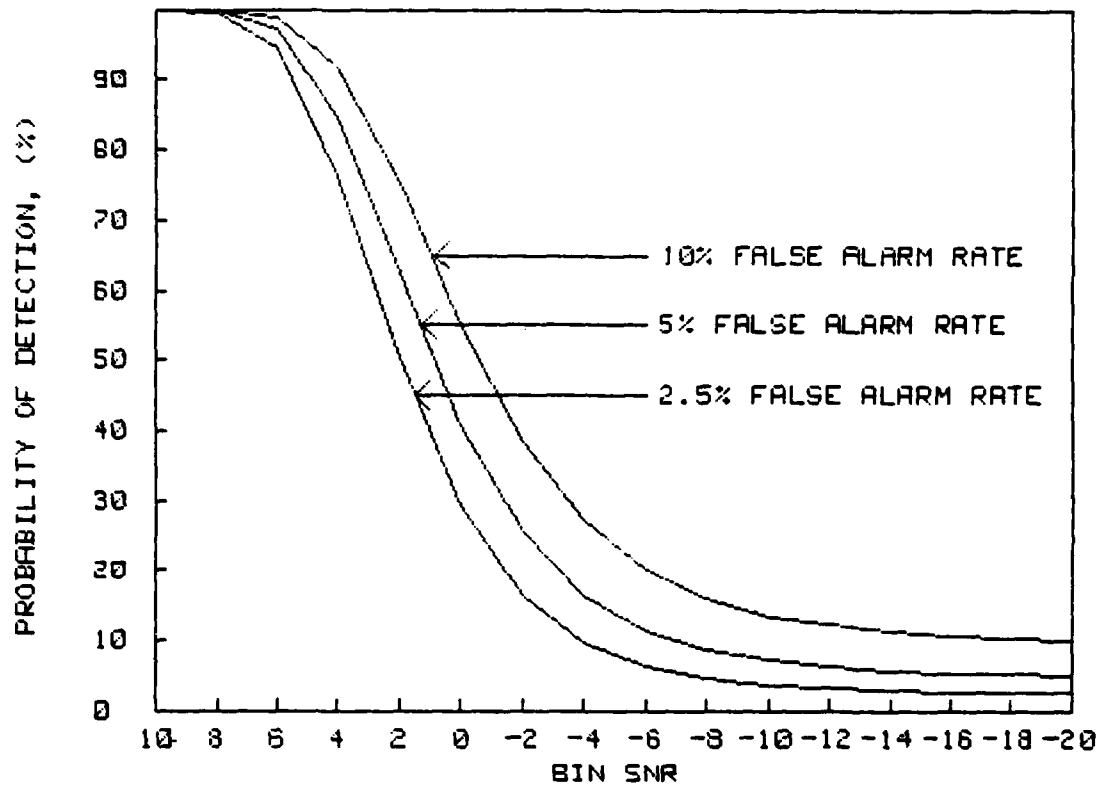


Fig. 17. Probability of detection vs. signal-to-noise ratio.

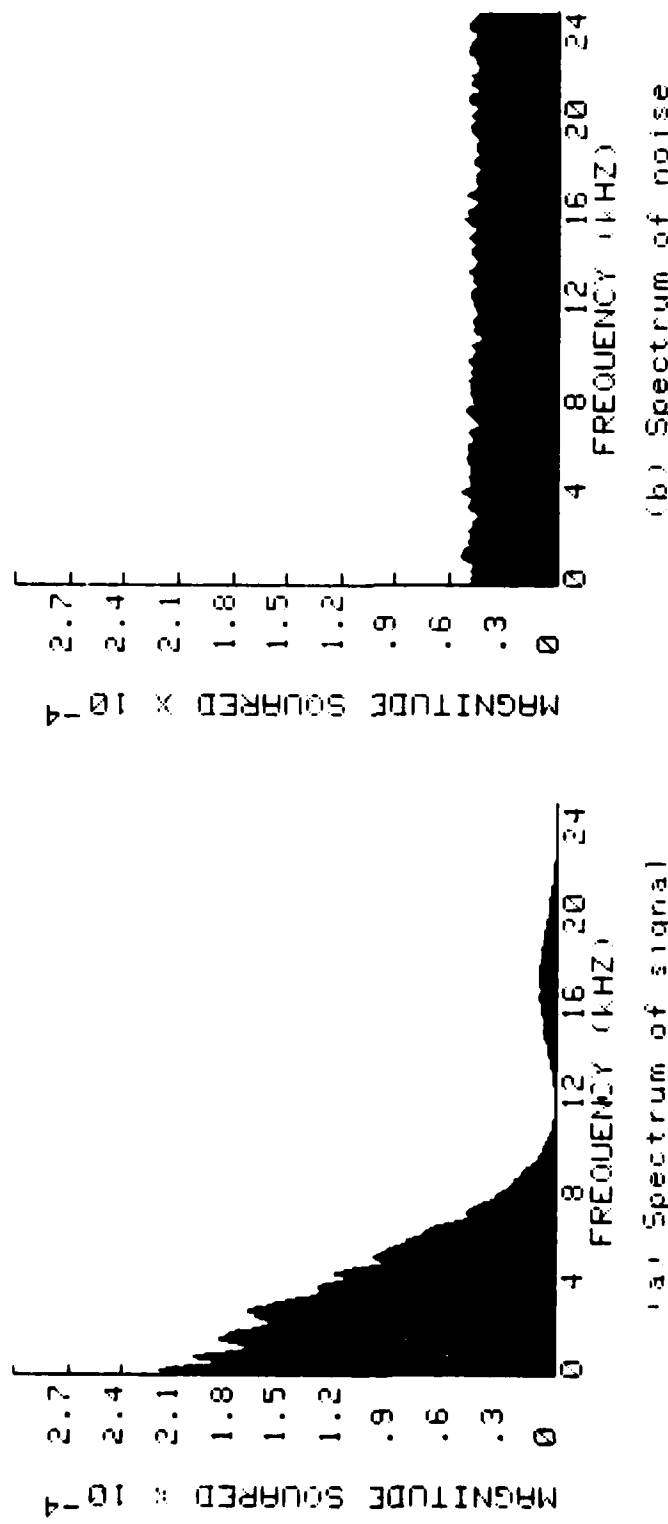
percent false alarm rates. Figs. 16 and 17, which are obtained from the equations derived in Appendix B, indicate the trade-offs involved using these detection methods.

B. WIDEBAND RESULTS

The FABLUS process makes decisions on a bin-by-bin basis, and so it can be applied to wideband signals having continuous spectra. To test this capability, a pseudo-random sequence of length 1,048,575 was used as a signal. Because a noise-like signal is used, the signal spectrum can only be specified on an average or mean basis. Fig. 18a shows the spectrum of the pseudo-random sequence based on an average over 500 data blocks. Fig. 18b shows the spectrum of the noise also based on 500 samples. The overall signal-to-noise ratio is 0 dB. The bin signal-to-noise ratio has maximum values of 7.5 dB in the main lobe and -6.8 dB in the first sidelobe.

For a given ensemble size the spectral estimate with noise can be no better than the signal only spectral estimate based on the same number of samples. Fig. 19a shows the average of the signal only spectrum when M is 8, and Fig. 19b shows the spectral estimate when noise is added for ensemble size $M = 8$. Figures 20a and 20b are these results when M is 16.

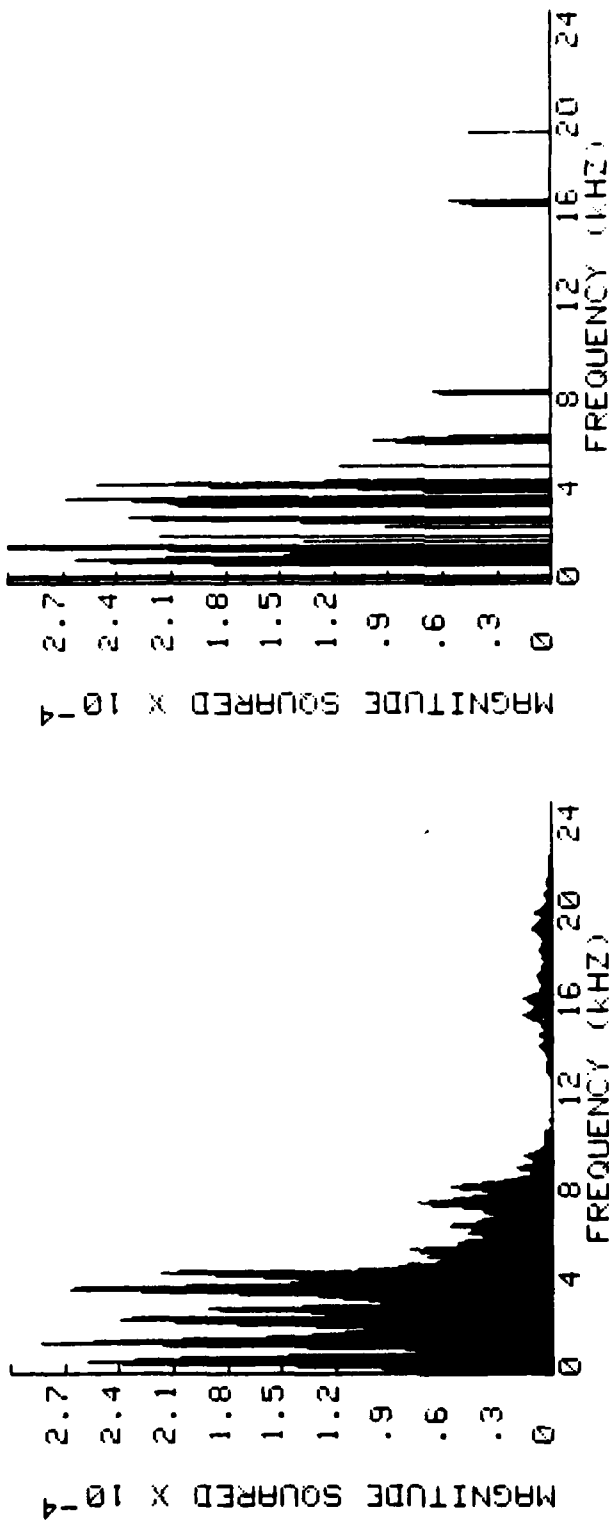
As expected the estimate for $M = 16$ is significantly better than for $M = 8$. In addition to showing less gaps in the main lobe area, the $M = 16$ estimate has considerably less variation in the amplitudes of the spectral components.



(b) Spectrum of noise

(a) Spectrum of signal

Fig.18. Spectrum of signal only and noise only based on an average of 500 data blocks.



(a.) Spectrum of the signal only, average of 8 data blocks
 (b.) Estimate of the spectrum with noise, ensemble size 8.

Fig. 19. Measured and estimated spectra; ensemble size of 8, composite signal-to-noise ratio of 0 dB.

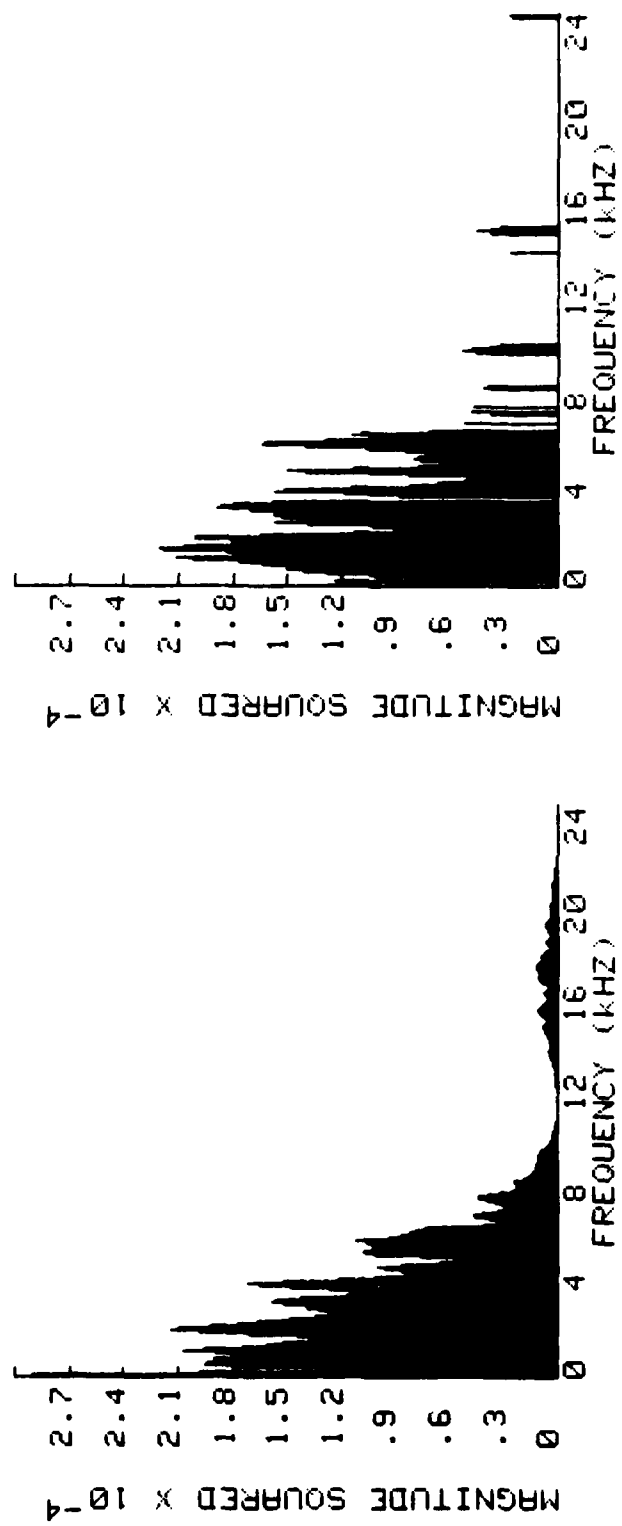


Fig. 20. Measured and estimated spectra; ensemble size of 16, composite signal-to-noise ratio of 0 dB.

Neither estimate shows significant components in the side-lobe area. This is caused by the low bin signal-to-noise ratio in the sidelobe area. At the peak of the sidelobe the bin signal-to-noise ratio is -6.8 dB. At this value, the probability of detection is 7.5 percent for $M = 16$.

V. CONCLUSIONS

The FABLUS process provides an estimate of the spectrum of an unknown signal. The process performs equally well with narrowband and wideband signals. Two implementations of the FABLUS process are evaluated. One method requires twice the memory capacity and additional processing time, but it produces marginally better probability of detection, and it requires the least restrictive assumptions about the signal spectrum. The accuracy of the estimate of the signal spectrum is limited only by the ensemble size and the inaccuracies inherent in the FFT process.

APPENDIX A
THE DISCRETE FOURIER TRANSFORM

1. Equations

A basic Fourier analysis result is that a periodic time function $x(t)$ can be represented by a sum of sinusoids of proper frequencies and amplitudes. This sum is the Fourier series [Ref. 6].

$$x(t) = A_0 + \sum_n (A_N \cos(2\pi nt/T) + B_N \sin(2\pi nt/T))$$

where T is the period of $x(t)$. If $x(t)$ is not periodic (or $T \rightarrow \infty$), then its frequency description becomes the Fourier transform represented mathematically as [Ref. 7]:

$$F(x(t)) = X(f) = \int_{-\infty}^{\infty} x(t) e^{-j2\pi ft} dt$$

The discrete Fourier transform (DFT) uses sample values of $x(t)$ obtained over a finite length of time (record length). The bandlimited, continuous time function $x(t)$ having Fourier transform $X(f)$ is first sampled at intervals of T seconds to produce the sampled time function $x(mT)$ where m is the set of integers. Now, let a finite record of a sampled time function be $x(iT)$, $i = 0, \dots, N-1$. The Discrete Fourier transform of $x(iT)$ is

$$X(q) = \sum_i [x(iT) [\cos(ia) - j\sin(ia)]]$$

where $a = 2\pi q/N$, $j = \sqrt{-1}$, $q = 0, \dots, N-1$. Here, i is a subset of m , the set of integers. Dropping the T for convenience and rearranging gives

$$X(q) = \sum_i [x(i)\cos(ia) - jx(i)\sin(ia)]$$

which has real and imaginary parts

$$\text{Re}[X(q)] = \sum_i x(i)\cos(ia)$$

$$\text{Im}[X(q)] = \sum_i x(i)\sin(ia).$$

The squared magnitude of the transform which is used in this report is

$$\begin{aligned} |X(q)|^2 &= [\sum_i x(i)\cos(ia)]^2 + [\sum_i x(i)\sin(ia)]^2 \\ &= \sum_{ij} x(i)x(j)\cos(ia)\cos(ja) + \\ &\quad \sum_{ij} x(i)x(j)\sin(ia)\sin(ja) \\ &= \sum_{ij} x(i)x(j)[\cos(ia)\cos(ja) + \\ &\quad \sin(ia)\sin(ja)] \end{aligned}$$

2. Errors

From the sampling theorem [Ref. 8], $x(mT)$ contains all the information necessary to reconstruct $x(t)$ if T is selected so that $1/T$ is at least twice the highest non-zero frequency component of $X(f)$. If $X(f)$ exists for $f > 1/2T$, aliasing

occurs which means the frequency components of $x(mT)$ are not the same as those of $x(t)$. This is the first source of error in the DFT.

Since $x(mT)$ contains an infinite number of values, for computational purposes we must truncate $x(mT)$ to some reasonable length. This truncation is accomplished by selecting some number N of samples to be considered. Therefore, the record length T_0 is NT . The truncation process is also called windowing because it is equivalent to multiplying $x(mT)$ by a window function. In the frequency domain the multiplication of these two time functions is equivalent to convolution of the spectrum of $x(mT)$ with the spectrum of the window function. Therefore, the spectrum of $x(mT)$ is altered by the window function. This is the second source of error in the DFT process.

To obtain the spectrum of $x(mT)$, the DFT assumes the available record repeats and calculates the Fourier transform using the sample values. This results in values for N terms at frequencies which are multiples of $1/T_0 = 1/NT = f_0$. This discrete spectrum $X(mf_0)$ may mask the maximum and minimum values of $X(f)$, the true spectrum of $x(t)$.

The DFT output, then, consists of N complex numbers representing the magnitudes and phases of the transform at the N frequencies spaced $1/NT$ Hz apart. However, only $N/2$ values of the transform are unique. The values from $N/2$ to N represent negative frequency components [Ref. 9]. Viewed from

another perspective, it is unreasonable to expect a linear process like the DFT to produce $2N$ linearly independent outputs (real and imaginary parts at N frequencies) with only N linearly independent inputs.

We can summarize these various effects by comparing the DFT output with a sampled version of $X(f)$.

Let $X'(mf_0)$ = the sampled version of $X(f)$

and let $X(mf_0)$ = the DFT output.

Then, $X(mf_0) = X'(mf_0) - Al(mf_0) - Tr(mf_0)$ where $Al(mf_0)$ represents the distortion in $X(mf_0)$ caused by aliasing and $Tr(mf_0)$ represents the distortion in $X(mf_0)$ caused by truncation. The aliasing and truncation effects can cause $X(mf_0)$ to increase or decrease.

The FFT is a computationally efficient algorithm used to generate the DFT values.

APPENDIX B

DERIVATION OF STATISTICAL PROPERTIES OF SINUSOIDAL SIGNAL AND UNCORRELATED, GAUSSIAN NOISE

In this appendix, we derive the equations for the mean and variance of the frequency bin squared magnitudes which are computed by the FABLUS process. The derivation considers the cases of noise only and sinusoid plus noise. That is, we derive here $E\{|G_N(p)|^2\}$, $\text{Var}\{|G_N(p)|^2\}$, $E\{|G_C(p)|^2\}$ and $\text{Var}\{|G_C(p)|^2\}$.

1. Noise Only

From Appendix A, if we let $x(i) = n(i) = \text{noise only}$ and let G_N represent the transform under noise only conditions, then

$$|G_N(p)|^2 = \sum_{ij} n(i)n(j) [\cos(ia)\cos(ja) + \sin(ia)\sin(ja)]$$

The expected value of the squared magnitude becomes:

$$E\{|G_N(p)|^2\} = \sum_{ij} \overline{n(i)n(j)} [\cos(ia)\cos(ja) + \sin(ia)\sin(ja)]$$

If $n(i)$ is independent from sample to sample and recognizing that the only random quantities are the $n(i)$, then the expected value is really the result of an ensemble average which becomes (assuming stationary noise).

$$\overline{n(i)n(j)} = 0 \quad \text{for } i \neq j$$

$$\begin{aligned}
 E\{|G_N(p)|^2\} &= \sum_i \overline{n(i)n(i)} [\cos^2(ia) + \sin^2(ia)] \\
 &= \overline{Nn(i)^2} \\
 &= \overline{Nn^2}
 \end{aligned}$$

Now, the squared value of the magnitude squared is

$$\begin{aligned}
 [|x(p)|^2]^2 &= \{ \sum_{ij} x(i)x(j) [\cos(ia)\cos(ja) + \sin(ia)\sin(ja)] \}^2 \\
 &= \sum_{ijkl} \{ x(i)x(j)x(k)x(l) [\cos(ia)\cos(ja) + \\
 &\quad \sin(ia)\sin(ja)] [\cos(ka)\cos(la) + \\
 &\quad \sin(ka)\sin(la)] \}
 \end{aligned}$$

If $x(i) = n(i)$ = noise only, then the mean square value becomes:

$$\begin{aligned}
 E\{[|G_N(p)|^2]^2\} &= \sum_{ijkl} \{ \overline{n(i)n(j)n(k)n(l)} [\cos(ia)\cos(ja) + \\
 &\quad \sin(ia)\sin(ja)] [\cos(ka)\cos(la) + \\
 &\quad \sin(ka)\sin(la)] \}
 \end{aligned}$$

If $n(i)$ is independent from sample to sample and again recognizing that the $n(i)$ are the only random quantities, then this expression has values only when $i = j = k = l$ or $i = j$ and $k = l$ or $i = k$ and $j = l$ or $i = l$ and $j = k$.

There will be N conditions when $i = j = k = 1$.

$$\begin{aligned}
 E\{[|G_N(p)|^2]^2\} &= \overline{\sum_i n(i)^4 [\cos^2(ia) + \sin^2(ia)] [\cos^2(ia) + \sin^2(ia)]} \\
 &+ \overline{\sum_{jk} n(j)n(j)n(k)n(k) [\cos^2(ja) + \sin^2(ja)] [\cos^2(ka) + \sin^2(ka)]} \\
 &+ \overline{\sum_{jk} n(j)n(k)n(j)n(k) [\cos(ja)\cos(ka) + \sin(ja)\sin(ka)]^2} \\
 &+ \overline{\sum_{jk} n(j)n(k)n(k)n(j) [\cos(ja)\cos(ka) + \sin(ja)\sin(ka)]^2}
 \end{aligned}$$

The cosine squared plus sine squared terms are unity and the use of the produce trionometeric identity yields:

$$\begin{aligned}
 E\{[|G_N(p)|^2]^2\} &= \overline{\sum_i n(i)^4} + \overline{\sum_{jk} n(j)n(j)n(k)n(k)} \\
 &+ \overline{\sum_{jk} \{[n(j)n(k)n(j)n(k)] + [n(j)n(k)n(k)n(j)]\} \{[\cos^2((j-k)a)]\}} \\
 &= \overline{\sum_i n(i)^4} + \overline{\sum_{jk} n(j)^2 n(k)^2} + \\
 &\quad 2 \overline{\sum_{jk} n(j)^2 n(k)^2 \cos^2((j-k)a)}
 \end{aligned}$$

$$\begin{aligned}
 E\{[|G_N(p)|^2]^2\} &= \overline{Nn^4} + (N^2 - N) \overline{(n^2)^2} + 2 \overline{(n^2)^2} \sum_{jk} \cos^2((j-k)a) \\
 &= \overline{Nn^4} + (2N^2 - 3N) \overline{(n^2)^2}
 \end{aligned}$$

Now, $\text{Var}(x) = E(x^2) - [E(x)]^2$. Therefore,

$$\begin{aligned}
 \text{Var}(|G_N(p)|^2) &= \overline{Nn^4} + (2N^2 - 3N) \overline{(n^2)^2} - N^2 \overline{(n^2)^2} \\
 &= \overline{Nn^4} + (N^2 - 3N) \overline{(n^2)^2}
 \end{aligned}$$

If $n(i)$ is Gaussian distributed then $\overline{n^4} = 3(\overline{n^2})^2$ and so $\text{Var}[|G_N(p)|^2] = N^2(\overline{n^2})^2$ which is a result used to define a signal-to-noise ratio in Chapter III.

2. Signal Plus Noise

If $x(i) = s(i) + n(i)$ = Signal plus Noise, then letting G_C represent the transform under signal plus noise conditions the expected value of the magnitude squared becomes:

$$\begin{aligned} E[|G_C(p)|^2] &= \sum_{ij} \overline{[s(i)+n(i)][s(j)+n(j)][\cos(ia)\cos(ja) \\ &\quad +\sin(ia)\sin(ja)]} \\ &= \sum_{ij} \overline{\{s(i)s(j)+s(i)n(j)+s(j)n(i)+n(i)n(j)\}[\cos(ia) \\ &\quad \cos(ja)+\sin(ia)\sin(ja)]} \end{aligned}$$

If $s(i)$ and $n(i)$ are independent, $\overline{n(i)} = 0$ and recognizing that the sine and cosine terms are not random gives

$$\begin{aligned} E[|G_C(p)|^2] &= \sum_{ij} \overline{s(i)s(j)[\cos(ia)\cos(ja)+\sin(ia)\sin(ja)]} \\ &\quad + \sum_{ij} \overline{n(i)n(j)[\cos(ia)\cos(ja)+\sin(ia)\sin(ja)]} \end{aligned}$$

From previous work, the second term equals $\overline{Nn^2(i)}$. If $s(i) = A\cos(2\pi fci/N)$, then $s(i)$ is deterministic, and we have by letting $F = 2\pi f/N$

$$\begin{aligned} E[|G_C(p)|^2] &= A^2 \sum_{ij} \overline{\cos(Fi)\cos(Fj)[\cos(ia)\cos(ja)+\sin(ia)\sin(ja)]} \\ &\quad + \overline{Nn^2} \end{aligned}$$

When $F \neq p$ this reduces to the noise only case.

For $F = p$ we have

$$E\{|G_C(p)|^2\} = A^2 N^2 / 4 + \overline{N^2}$$

Now consider the value of the squared magnitude squared:

$$\begin{aligned} \{|x(p)|^2\}^2 &= \sum_{ijkl} \{x(i)x(j)x(k)x(l) [\cos(ia)\cos(ja) + \sin(ia)\sin(ja)] \\ &\quad [\cos(ka)\cos(la) + \sin(ka)\sin(la)] \} \end{aligned}$$

For $x(i) = s(i) + n(i)$ we get:

$$\begin{aligned} \{|G_C(p)|^2\}^2 &= \sum_{ijkl} \{[s(i)+n(i)][s(j)+n(j)][s(k)+n(k)][s(l)+n(l)] \\ &\quad [\cos(ia)\cos(ja) + \sin(ia)\sin(ja)] \\ &\quad [\cos(ka)\cos(la) + \sin(ka)\sin(la)] \} \end{aligned}$$

Now, the expected value of the squared magnitude squared becomes:

$$\begin{aligned} E\{|G_C(p)|^2\}^2 &= \sum_{ijkl} \{ \overline{s(i)s(j)s(k)s(l)} + \overline{s(i)s(k)n(j)n(l)} + \\ &\quad \overline{n(i)s(j)s(k)s(l)} + \overline{n(i)n(j)s(k)s(l)} + \\ &\quad \overline{s(i)s(j)n(k)s(l)} + \overline{s(i)n(j)n(k)s(l)} + \\ &\quad \overline{n(i)s(j)n(k)s(l)} + \overline{n(i)n(j)n(k)s(l)} + \\ &\quad \overline{s(i)s(j)s(k)n(l)} + \overline{s(i)s(k)n(j)n(l)} + \\ &\quad \overline{n(i)s(j)s(k)n(l)} + \overline{n(i)n(j)s(k)n(l)} + \\ &\quad \overline{s(i)s(j)n(k)n(l)} + \overline{s(i)n(j)n(k)s(l)} + \\ &\quad \overline{n(i)s(j)n(k)n(l)} + \overline{n(i)n(j)n(k)n(l)} \} \\ &\quad [\cos(ia)\cos(ja) + \sin(ia)\sin(ja)] \\ &\quad [\cos(ka)\cos(la) + \sin(ka)\sin(la)] \end{aligned}$$

If $n(i)$ has zero mean and zero third moment, and if $n(i)$ is independent of $s(i)$, and if $s(i)$ is deterministic, and recognizing that only $n(i)$ is random, then

$$\begin{aligned} E\{[|G_C(p)|^2]^2\} &= \sum_{ijkl} [s(i)s(j)s(k)s(l) + \overline{n(i)n(j)s(k)s(l)} + \\ &\quad \overline{s(i)n(j)n(k)s(l)} + \overline{n(i)s(j)n(k)s(l)} + \\ &\quad \overline{s(i)s(k)n(j)n(l)} + \overline{n(i)s(j)s(k)n(l)} + \\ &\quad \overline{s(i)s(j)n(k)n(l)} + \overline{n(i)n(j)n(k)n(l)}] \\ &\quad [\cos(ia)\cos(ja) + \sin(ia)\sin(ja)] \\ &\quad [\cos(ka)\cos(la) + \sin(ka)\sin(la)] \end{aligned}$$

Assuming $n(i)n(j) = 0$ for $i \neq j$ (sample to sample independence), then

$$\begin{aligned} E\{[|G_C(p)|^2]^2\} &= \sum_{ijkl} [s(i)s(j)s(k)s(l) [\cos(ia)\cos(ja) + \\ &\quad \sin(ia)\sin(ja)] [\cos(ka)\cos(la) + \\ &\quad \sin(ka)\sin(la)] \\ &\quad + 2 \sum_{ijk} \overline{n(i)^2 s(j)s(k) [\cos^2(ia) + \sin^2(ia)]} \\ &\quad [\cos(ja)\cos(ka) + \sin(ja)\sin(ka)] \\ &\quad + 4 \sum_{ijk} \overline{n(i)^2 s(j)s(k) [\cos(ia)\cos(ja) + \\ &\quad \sin(ia)\sin(ja)] [\cos(ka)\cos(ia) + \\ &\quad \sin(ka)\sin(ia)]} \\ &\quad + \sum_{ijkl} \overline{n(i)n(j)n(k)n(l) [\cos(ia)\cos(ja) + \\ &\quad \sin(ia)\sin(ja)] [\cos(ka)\cos(la) + \\ &\quad \sin(ka)\sin(la)]} \end{aligned}$$

Assuming $s(i) = A \cos(Fi)$ where $F = 2\pi f c/N$ and $n(i)$ is Gaussian, then

$$\begin{aligned} E[|G_C(p)|^2]^2 &= A^4 N^4 / 16 + 2[A^2 N^3 \overline{n^2} / 4] + 4[A^2 N^3 \overline{n^2} / 8] \\ &\quad + 2N^2 (\overline{n^2})^2 \\ &= A^4 N^4 / 16 + A^2 N^3 \overline{n^2} / 2 + N^2 (\overline{n^2})^2 \end{aligned}$$

Now, $\text{Var}(x) = E[x^2] - [E(x)]^2$. Therefore,

$$\text{Var}[|G_C(p)|^2]^2 = A^2 N^3 \overline{n^2} / 2 + N^2 (\overline{n^2})^2$$

APPENDIX C

PROBABILITY OF DETECTION FOR SINUSOIDAL SIGNAL AND UNCORRELATED, GAUSSIAN NOISE

Using the assumptions for Method I in Chapter III, the probability of detection is

$$P_d = P(r > C_v)$$

where r is the decision variable and C_v is the critical value.

From Appendix B for the case of white, Gaussian noise and sinusoidal signal,

$$\overline{|G_N|^2} = N\overline{n^2},$$

$$\text{var}(|G_N|^2) = N^2(\overline{n^2})^2,$$

$$\overline{|G_C|^2} = A^2 N^2/4 + N\overline{n^2},$$

$$\text{var}(|G_C|^2) = A^2 N^3 \overline{n^2}/2 + N^2(\overline{n^2})^2.$$

Therefore, the decision variable become

$$\begin{aligned} R &= \overline{|G_C|^2} - \overline{|G_N|^2} \\ &= A^2 N^2/4 + N\overline{n^2} - N\overline{n^2} \\ &= A^2 N^2/4 \end{aligned}$$

and

$$\begin{aligned}
 s_S^2 &= (A^2 N^3 \bar{n}^2 / 2 + N^2 (\bar{n}^2)^2 + N^2 (\bar{n}^2)^2) / M \\
 &= (A^2 N^3 \bar{n}^2 + 4N^2 (\bar{n}^2)^2) / 2M \\
 s_S &= \sqrt{((A^2 N^3 \bar{n}^2 + 4N^2 (\bar{n}^2)^2) / 2M)}.
 \end{aligned}$$

The critical value is:

$$\begin{aligned}
 Cv &= z_\alpha s_S \\
 &= z_\alpha \sqrt{((A^2 N^3 \bar{n}^2 + 4N^2 (\bar{n}^2)^2) / 2M)}.
 \end{aligned}$$

Using the above expressions,

$$\begin{aligned}
 Pd &= P(r | v-u = A^2 N^2 / 4) \\
 &= Q((Cv - R) / s_S) \\
 &= Q(z_\alpha - (A^2 N^2 \sqrt{M}) / (4 \sqrt{(N^3 A^2 \bar{n}^2 / 2 + 2N^2 (\bar{n}^2)^2)}))).
 \end{aligned}$$

LIST OF REFERENCES

1. Dicke, R. H., "The Measurement of Thermal Radiation at Microwave Frequencies," REV. SCI. INSTR., Vol 17, p. 268-275, July 1946.
2. Miller, Irwin and Freund, J. E., Probability and Statistics for Engineers, 2d ed., p. 170, Prentice-Hall, 1977.
3. Hoel, P. G. and Jessen, R. J., Basic Statistics for Business and Economics, 2d ed., p. 160, John Wiley, 1977.
4. Op. Cit., Miller and Freund, p. 346.
5. Op. cit., Hoel and Jessen, p. 226.
6. Stremler, F. G., Introduction to Communications Systems, p. 30, Addison-Wesley, 1977.
7. Ibid., p. 32.
8. Oppenheim, A. V. and Schafer, R. W., Digital Signal Processing, p. 29, Prentice-Hall, 1975.
9. Op. cit., Stremler, p. 130.

INITIAL DISTRIBUTION LIST

	No. Copies
1. Defense Technical Information Center Cameron Station Alexandria, Virginia 22311	2
2. Library, Code 0142 Naval Postgraduate School Monterey, California 93940	2
3. Prof. Glen A. Myers, Code 62Mv Department of Electrical Engineering Naval Postgraduate School Monterey, California 93940	10
4. Prof. Stephen Jauregui, Code 62Ja Department of Electrical Engineering Naval Postgraduate School Monterey, California 93940	1
5. Lieutenant Michael Davis, USN Naval Electronics Systems Engineering Center P. O. Box 80337 San Diego, California 92138	1
6. Mr. Alan J. Howarth 9630 Erie Street Highland, Indiana 46322	1
7. Lieutenant Commander G. L. Howarth, USN 5553 Ann Peake Drive Fairfax, Virginia 22032	2
8. Captain Henry Orejuela, USN Naval Electronic Systems Command PME-107-9 Washington, D.C. 20360	1

DATE
ILMED
- 8